**ORIGINAL ARTICLE**

# Nekhoroshev estimates for the orbital stability of Earth's satellites

Alessandra Celletti[1] · Irene De Blasi[2] · Christos Efthymiopoulos[3]

## Abstract

We provide stability estimates, obtained by implementing the Nekhoroshev theorem, in reference to the orbital motion of a small body (satellite or space debris) around the Earth. We consider a Hamiltonian model, averaged over fast angles, including the $J_2$ geopotential term as well as third-body perturbations due to Sun and Moon. We discuss how to bring the Hamiltonian into a form suitable for the implementation of the Nekhoroshev theorem in the version given by Pöschel, (Math Z 213(1):187–216, 1993) for the 'non-resonant' regime. The manipulation of the Hamiltonian includes (i) averaging over fast angles, (ii) a suitable expansion around reference values for the orbit's eccentricity and inclination, and (iii) a preliminary normalization allowing to eliminate particular terms whose existence is due to the nonzero inclination of the invariant plane of secular motions known as the 'Laplace plane'. After bringing the Hamiltonian to a suitable form, we examine the domain of applicability of the theorem in the action space, translating the result in the space of physical elements. We find that the necessary conditions for the theorem to hold are fulfilled in some nonzero measure domains in the eccentricity and inclination plane $(e, i)$ for a body's orbital altitude (semimajor axis) up to about 20 000 km. For altitudes around 11 000 km, we obtain stability times of the order of several thousands of years in domains covering nearly all eccentricities and inclinations of interest in applications of the satellite problem, except for narrow zones around some so-called inclination-dependent resonances. On the other hand, the domains of Nekhoroshev stability recovered by the present method shrink in size as the semimajor axis $a$ increases (and the corresponding Nekhoroshev times reduce to hundreds of years), while the stability domains practically all vanish for $a > 20 000$ km. We finally examine the effect on Nekhoroshev stability by adding more geopotential terms ($J_3$ and $J_4$) as well as the second-order terms in $J_2$ in the Hamiltonian. We find that these terms have only a minimal effect on the domains of applicability of Nekhoroshev theorem and a moderate effect on the stability times.

✉ Irene De Blasi
  irene.deblasi@unito.it

1   Department of Mathematics, University of Rome Tor Vergata, Rome, Italy

2   Department of Mathematics, University of Torino, Torino, Italy

3   Department of Mathematics, University of Padova, Padova, Italy

# 1 Introduction

The study of the stability of the motion of celestial bodies is relevant from both the theoretical and practical points of view; such investigation can be approached using numerical or analytical tools (see (Celletti 2010) for a review). In this work, we consider the problem of the long-term (over $10^3$–$10^4$ years) stability of a small body (satellite or space debris) in orbit around the Earth and subject to third-body perturbations due to the Moon and the Sun. By stability, we mean that the body undergoes no large variations of its orbital elements that could produce a drastic change (e.g., escape) in the orbit.

In the orbital study of satellite motions, it is convenient to split the space environment around the Earth into three distinct regions according to the distance from the Earth's surface, where different elements can affect the dynamics:

- ($i$) LEO: Low-Earth-Orbit (from 90 to 2000 km of altitude), where the Earth's atmosphere generates dissipative effects;
- ($ii$) –($iii$) MEO: Medium-Earth-Orbit (between 2000 and 30 000 km of altitude) and GEO: Geostationary-Earth-Orbit (altitudes around the geosynchronous orbit at about 35 786 km), where the dissipative effect of the atmosphere is negligible and the dynamical system associated with the equations of motion is conservative. In these regimes, the most important contributions are due to the geopotential and to the lunar and solar third-body perturbations.

We will hereafter consider a Hamiltonian model for the motion of small bodies at MEO (see, instead, Celletti and Galeş 2018; Lhotka et al. 2016 for the inclusion of dissipative effects). The study of dynamics at MEO in the conservative regime has been subject of many works, including the development of analytical models (e.g., Celletti and Gales 2014; Celletti et al. 2017; Giacaglia 1974; Kaula 1962; Lane 1989), study of resonances (e.g., Breiter 2001a, b; Celletti et al. 2020, 2016, 2017; Chao and Gick 2004; Cook 1962; Ely and Howell 1997; Hughes 1980; Lemaître et al. 2009), as well as the dynamical chartography (stability maps, onset of chaos) of the MEO region (e.g., Alessi et al. 2016; Casanova et al. 2015; Daquin et al. 2016; Gkolias et al. 2016; Rosengren and Scheeres 2013; Rosengren et al. 2015, 2016; Rossi 2008; Skoulidou et al. 2019; Valk and Lemaître 2008).

The aim of this work is to study the stability of a model for objects in MEO from an analytical point of view, providing exponential stability estimates using the celebrated *Nekhoroshev theorem* (Nekhoroshev 1977). We stress that, while the Nekhoroshev theorem is particularly relevant for systems with three or more degrees of freedom, which can be affected by the phenomenon known as *Arnold diffusion* (Arnold 1964), the applicability of the theorem in securing the long-term stability in *open domains* in the action space holds for systems of any number of degrees of freedom larger than or equal to two. Furthermore, the Nekhoroshev theorem was originally developed under a suitable non-degeneracy condition, called *steepness*, while later approaches (e.g. Benettin and Gallavotti 1986; Pöschel 1993) focus on the important subcase of convex and quasi-convex Hamiltonians (see Pöschel 1993 for definitions). As regards the applications, the theorem was proved useful in obtaining realistic estimates of the domains or times of practical stability of the orbits in a number of interesting problems in Celestial Mechanics. Among others, we mention the three-body problem (Cel-

letti and Ferrara 1996) as well as the problem of the Trojan asteroids (Celletti and Giorgilli 1991; Giorgilli and Skokos 1997).

In this work, we apply the Nekhoroshev theorem to a model approximating the (averaged over short period terms) dynamics of a small body around the Earth. As discussed below, this allows to obtain long-time stability estimates for realistic sets of parameters, at least for altitudes (values of the semimajor axis) below 20 000 km.

Our main model, explained in detail in Sect. 2, is ruled by a Hamiltonian function obtained as the sum of different contributions, namely the geopotential $J_2$ term as well as the third-body perturbations on the small body by the Sun and Moon. We assume the spatial case of the small body's motion, while we approximate the Moon's and Sun's orbits as fixed Keplerian ellipses lying in the ecliptic plane. We argue (Sect. 2) that the Moon's precession of the nodes introduces only minimal effects as regards the problem of determining Nekhoroshev stability, due to the fact that the frequency of the precession is much smaller than any of the frequencies in the small body's motion. As a result, our point of departure is a Hamiltonian model obtained by a 3 degrees of freedom and time-dependent Hamiltonian function, which depends quasi-periodically on time, since the (fast) frequencies of motion of the Sun and Moon are non-commensurable.

Now, as discussed in Sect. 2, this model is still not convenient for the discussion of Nekhoroshev stability over secular timescales, because both short and long period effects are included in it. Working, however, with closed-form perturbation theory (namely, without series expansions in eccentricity and inclination, see Lara 2021; Brouwer 1959 for a review), one can eliminate all short-period terms and arrive at an autonomous Hamiltonian with two degrees of freedom which is convenient for the description of the secular motions of the small body. As our basic model, we then adopt the one found after averaging (in closed-form) over the Earth's $J_2$ term and the Sun's and Moon's quadrupolar ($P_2$) terms. Several studies (see Daquin et al. 2016; Gkolias et al. 2016; Aristoff et al. 2021; Nie and Gurfil 2021 and references therein) have demonstrated the relevance of this model in capturing all important effects for the long-term dynamics at MEO. In Sect. 5, however, we consider also a more complicated model including the Earth's $J_3$ and $J_4$ terms to first order, as well as $J_2^2$ terms. The latter are computed by implementing a *closed form* averaging through Deprit's elimination of the parallax technique (Deprit 1982; Lara et al. 2020, 2014). One finds (see the discussion in Sect. 5) that the relative importance of these terms over lunisolar terms decreases with altitude; yet, these terms provide relevant contributions to the Hamiltonian for the lowermost altitudes considered in the present work (namely, with semimajor axis $a \approx 11\,000$ km).

After fixing the initial model, an important aspect of our present work concerns a number of preliminary operations performed on the initial Hamiltonian, which turn to be crucial to the purpose of bringing the Hamiltonian in a form allowing to explicitly demonstrate the fulfillment of the conditions for the holding of the Nekhoroshev theorem in the form given in Pöschel (1993). These preliminary steps are explained in detail in Sect. 2 below and can be summarized as follows:

(i) *Average over fast angles.* We start by averaging the Hamiltonian over the problem's fast angles, i.e., the mean anomalies of the small body's, Moon's and Sun's orbits. After this operation, the semimajor axis $a$ of any orbit becomes a constant which can be used to label the altitude of each orbit.

(ii) *Expansion around reference values in the eccentricity and inclination.* The remaining elements (eccentricity $e$ and inclination $i$), which can be mapped into the action variables of the problem, undergo 'secular' (slow) evolution under the averaged Hamiltonian. Our

purpose is to characterize the stability of the orbits in the space $(e, i)$ of the orbital elements. To this end, fixing a grid of reference values $(e_*, i_*)$ in the plane $(e, i)$ for each (constant) semimajor axis $a = a_*$, we perform a Taylor expansion of the averaged Hamiltonian around the points in action space associated with the reference point $(e_*, i_*)$. This step is important, since the Taylor-expanded Hamiltonian can be easily manipulated in terms of normalizing canonical transformations necessary to perform with the aid of a computer-algebraic program (see below).

(iii) *Preliminary normalization*. We perform a preliminary normalization of the averaged and Taylor-expanded Hamiltonian, aiming to eliminate some terms which, albeit reflecting a trivial dynamics (see Sect. 3), may artificially affect the estimates found by implementing Pöschel's version of the Nekhoroshev theorem. We argue below that this step is a consequence of the nonzero value of the inclination of the Laplace plane with respect to the Earth's equatorial plane. The inclination can be expressed as

$$i^{(p)} \simeq -\frac{A}{2B} \frac{1}{(\mu_E a)^{1/4}} \tag{1}$$

where

$$
\begin{aligned}
A &= -\frac{3R_E^2 a^{7/4} \sin(2i_0)}{8(\mu_E)^{1/4}} \left( \frac{\mu_M}{a_M^3} + \frac{\mu_\odot}{a_\odot^3} \right), \\
B &= \frac{3}{4} \frac{\sqrt{\mu_E} R_E^2 J_2}{a^{7/2}} + \frac{3\mu_M(2 - 3\sin^2 i_0)}{16\sqrt{\frac{\mu_E}{a^3}} a_M^3} + \frac{3\mu_\odot(2 - 3\sin^2 i_0)}{16\sqrt{\frac{\mu_E}{a^3}} a_S^3}
\end{aligned}
\tag{2}
$$

with $R_E, \mu_E$ being the Earth's mean radius and mass parameter, $a_M, \mu_M$ are the Moon's semimajor axis and mass parameter, $a_\odot, \mu_\odot$ are the Sun's semimajor axis and mass parameter, and finally $i_0$ is the inclination of the ecliptic plane. A key result in the present paper is the use of normal form techniques to reduce the size, in the Hamiltonian, of all terms related to the Laplace plane (see Sect. 3); whenever convergent, this procedure is crucial to put the initial Hamiltonian in a form for which Nekhoroshev's non-resonant stability estimates can be produced, since it allows us to control the norm of the perturbing function under a suitable choice of the domain in the actions.

Now, following steps (i) to (iii) above, the procedure leads to a normalized 2 degrees of freedom Hamiltonian expressed in suitably defined action-angle variables $(\mathbf{I}, \mathbf{u}) \in \mathbb{R}^2 \times \mathbb{T}^2$, of the form:

$$\mathcal{H}(\mathbf{I}, \mathbf{u}) = h_0(\mathbf{I}) + h_1(\mathbf{I}, \mathbf{u}). \tag{3}$$

Using the Hamiltonian (3), we can derive stability results on the eccentricity and the inclination by implementing the estimates provided in Proposition 1 of Pöschel (1993). This proposition refers to the so-called *non-resonant* regime, i.e., when the fundamental frequencies deduced by the integrable part of the Hamiltonian, $h_0$, are subject to no resonance conditions. Under particular assumptions on the non-resonance condition for $h_0$, as well as on the smallness of the norm of $h_1$ in a suitable functional space and domain in the action variables (see Sect. 3.1), one can prove that the actions remain in a small neighborhood of their initial values for a period of time which is exponentially long with respect to the norm of $h_1$. We remark that Proposition 1 in Pöschel (1993) does not require any convexity assumption on the Hamiltonian. This assumption is relevant when analyzing resonant regimes (for a thorough analysis of different non-degeneracy conditions such as convexity, quasi-convexity, 3-jet, etc., see De Blasi et al. 2021). However, we also stress that, despite

**Table 1** Inclination-dependent resonances of order $\leq 4$ in the lunisolar model. The coefficients are such that $\alpha\dot{\omega} + \beta\dot{\Omega} = 0$, where $\omega$ is the argument of the perigee and $\Omega$ is the longitude of the ascending node (Hughes 1980)

| $\alpha$ | $\beta$ | $i(deg)$ | $\alpha$ | $\beta$ | $i(deg)$ | $\alpha$ | $\beta$ | $i(deg)$ | $\alpha$ | $\beta$ | $i(deg)$ |
|---|---|---|---|---|---|---|---|---|---|---|---|
| 1 | 0 | 63.43 | 0 | 1 | 90 | 1 | 1 | 46.37 | 1 | −1 | 73.1 |
| 2 | 1 | 56 | 1 | 2 | 0 | 2 | −1 | 69 | −1 | 12 | 78 |
| 3 | 1 | 58.75 | 3 | −1 | 67.33 | 1 | −3 | 81.47 | | | |

our use of Pöschel's proposition in the non-resonant regime, the presence of resonances at MEO plays an important role also in our results, as becomes evident in the discussion of our results in Sect. 4. In fact, we find that our obtained stability domains typically exclude some zones around the so-called *inclination-dependent resonances* (Hughes 1980), i.e., resonances appearing for particular values of the inclination of the orbit, independently of the value of the semimajor axis or the eccentricity. This is because the series constructed in our preliminary normalization of the Hamiltonian are affected by small divisors related to the most important of these resonances, given in Table 1. Also, the frequencies associated with these divisors influence the determination of the so-called Fourier cut-off (Sect. 3) which appears in the implementation of the Proposition 1 of Pöschel (1993).

As described in Sect. 4, the stability estimates obtained in this work strongly depend on the distance of the small body from the Earth's center: our results show that the domain of Nekhoroshev stability in the plane $(e, i)$ has a large volume (limited only by narrow strips around resonances) at the distance of 10 000 km, while it shrinks to a near-zero volume beyond the distance of 20 000 km. We should stress that this result is partly due to the dynamics itself (the secular—averaged over the fast angles - $J_2$ dynamics alone is integrable, but the third-body perturbations increase in relative size as the distance from the Earth increases), but also probably due, in part, to our particular technique used to apply the Nekhoroshev theorem, i.e. including the processing of the Hamiltonian as described in steps (i)–(iii) above. We thus leave open the possibility that this latter constraint be relaxed with the use of a better technique. Also, our present treatment is simplified in that we ignore the periodic oscillation of the Moon's line of nodes (by an amplitude of $11.5°$ over a period of 18.6 y) and inclination (by $\pm 5°$) around the ecliptic of the Moon's orbit with respect to the Earth's equatorial plane. This oscillation introduces one more secular frequency to the problem; however, it substantially affects the orbits only for semimajor axes $a > 20\,000$ km, which is, anyway, beyond the domain of stability presently found even while ignoring this effect.

As a final remark, in De Blasi et al. (2021) we studied the satellite's stability in two different models: the $J_2$ approximation of the geopotential and a model that includes $J_2$, Sun and Moon. We computed suitable normal forms and obtained stability results by estimating the size of the remainder function after the normalizing transformation. In De Blasi et al. (2021), we only considered values of the eccentricity and inclination close to zero and to the inclination of the Laplace plane, respectively. In terms of Table 1 above, this corresponds to the case of the $g + 2h$ resonance. Correspondingly, our stability estimates in De Blasi et al. (2021) were not obtained separately for eccentricity and inclination, but only as regards their combination $\sqrt{1 - e^2}\cos i$ through the Lidov-Kozai integral, which is the second integral associated with the $g + 2h$ resonance. This is a main difference with respect to the present paper, in which we consider generic values for the eccentricity and inclination far from any lunisolar resonance.

This article is organized as follows: Sect. 2 provides the construction of the secular Hamiltonian function which describes the model, as well as its normalization; in Sect. 3, the theoretical framework is described, along with the algorithm used to produce the normalized Hamiltonian and the stability estimates. Sect. 4 describes the results based on the Hamiltonian including the geopotential $J_2$ term and the third-body perturbations due to the Sun and Moon; Sect. 5 discusses the influence on Nekhoroshev stability by extending the model and including the $J_2^2$, $J_3$ and $J_4$ terms in the secular Hamiltonian. Finally, Sect. 6 summarizes the conclusions from the present work.

## 2 Hamiltonian preparation

In this Section, we provide details on the model (Sect. 2.1), on the corresponding secular Hamiltonian function averaged over fast angles (Sect. 2.2), the expansion around some reference values for the eccentricity and inclination (Sect. 2.3), and the preliminary normalization to remove specific terms (Sect. 2.4).

### 2.1 Model

We consider a small body (satellite or debris) $S$ of infinitesimal mass, under the action of the Earth's gravitational field and the third-body perturbations due to the Moon and Sun. Geocentric inertial Cartesian coordinates are denoted by $(x, y, z)$, where the $xy$-plane coincides with the Earth's equatorial plane, $z$ points to the north pole, and $x$ points to a fixed direction (ascending node of the Sun's geocentric orbit). We denote by $\mathbf{r}(t) = (x(t), y(t), z(t))$ the time-evolving radius vector of the body $S$, and by $(a, e, i, M, \omega, \Omega)$ the osculating orbital elements of $S$, where $a$ is the semimajor axis, $e$ is the eccentricity, $i$ is the inclination with respect to the Earth's equatorial plane, $M$ is the mean anomaly, $\omega$ is the argument of the perigee and $\Omega$ is the longitude of the ascending node.

In the sequel, we consider the following approximation to the body's equations of motion:

$$\ddot{\mathbf{r}} = -\nabla V_E(\mathbf{r}) - \mu_\odot \left( \frac{\mathbf{r} - \mathbf{r}_\odot}{|\mathbf{r} - \mathbf{r}_\odot|^3} + \frac{\mathbf{r}_\odot}{|\mathbf{r}_\odot|^3} \right) - \mu_M \left( \frac{\mathbf{r} - \mathbf{r}_M}{|\mathbf{r} - \mathbf{r}_M|^3} + \frac{\mathbf{r}_M}{|\mathbf{r}_M|^3} \right), \qquad (4)$$

where $V_E(\mathbf{r})$ approximates the geopotential via the relation

$$V_E(\mathbf{r}) = V_{kep}(|\mathbf{r}|) + V_{J_2}(\mathbf{r}), \qquad (5)$$

where $V_{kep}(r) = -\frac{\mu_E}{r}$ and $V_{J_2}$ in spherical coordinates $(r, \varphi, \phi)$ is given by[1]

$$V_{J_2}(r, \varphi, \phi) = \frac{\mu_E J_2}{r} \left\{ \left( \frac{R_E}{r} \right)^2 \left( \frac{3}{2} \sin^2 \phi - \frac{1}{2} \right) \right\}. \qquad (6)$$

In the above formulas:

- $\mathcal{G}$ is the gravitational constant, $\mu_E = \mathcal{G}m_E$, $\mu_M = \mathcal{G}m_M$, $\mu_\odot = \mathcal{G}m_\odot$ with $m_E$, $m_M$, $m_\odot$ the masses of the Earth, Moon and Sun, respectively.

---

[1] In the present section, as well as in Sects. 3 and 4, we limit our analysis to the $J_2$-term, which is the dominant term of the Earth's potential at all altitudes; however, in Sect. 5, we will discuss the influence on our results by the terms $J_3$, $J_4$, and $J_2^2$ (obtained through a canonical transformation), which become relevant for the lowermost limit in altitude of the MEO domain.

- We adopt the value $J_2 = 1.082 \times 10^{-3}$ for the $J_2$ coefficient, and $R_E = 6\,400$ km for the Earth's equatorial radius.
- $\mathbf{r}$, $\mathbf{r}_\odot$ and $\mathbf{r}_M$ are, respectively, the geocentric position vectors of $S$, Sun and Moon.

The expressions of $\mathbf{r}_\odot$ and $\mathbf{r}_M$ depend on the assumptions on the orbits of Sun and Moon. In this work, the geocentric orbit of the Sun is taken as a fixed ellipse with $a_\odot = 1.496 \times 10^8$ km, $e_\odot = 0.0167$ and $i_\odot = 23.44°$, while the geocentric orbit of the Moon is taken as a fixed ellipse with orbital parameters $a_M = 384\,748$ km, $e_M = 0.0554$ and $i_M = i_\odot{}^2$. The last assumption has an important effect on the dynamics: it implies that the only lunisolar resonances which affect the dynamics of the body are those whose location in the element space $(a, e, i)$ depends only on the inclination (see Hughes 1980). More resonances, instead, appear when the effect of nodal precession (by a period of 18.6 years) of the Moon's orbit is taken into account. However, these resonances affect the dynamics only at altitudes exceeding the ones where we presently establish Nekhoroshev stability (see Gkolias et al. 2016 and Sect. 4 below); thus, they can be ignored in the framework of our present study.

The Hamiltonian function which describes the motion of $S$ can be expressed as the sum of three contributions:

$$\mathcal{H} = \mathcal{H}_E + \mathcal{H}_\odot + \mathcal{H}_M, \tag{7}$$

where $\mathcal{H}_E = \mathbf{p}^2/2 + V_E(\mathbf{r})$ with $\mathbf{p} = \dot{\mathbf{r}}$, and $\mathcal{H}_\odot$ and $\mathcal{H}_M$ are the solar and lunar third-body perturbation terms. Considering the quadrupolar expansion of the third-body perturbation terms in the equations of motion (4), we find

$$
\begin{aligned}
\mathcal{H}_\odot = V_\odot(\mathbf{r}) &= -\frac{\mu_\odot}{|\mathbf{r} - \mathbf{r}_\odot|} + \frac{\mu_\odot}{r_\odot^3}\mathbf{r} \cdot \mathbf{r}_\odot \\
&= -\frac{\mu_\odot}{r_\odot} - \frac{\mu_\odot}{2r_\odot^3}r^2 + \frac{3}{2}\frac{\mu_\odot(\mathbf{r} \cdot \mathbf{r}_\odot)^2}{r_\odot^5} + O\left(\left(\frac{r}{r_\odot}\right)^3\right),
\end{aligned} \tag{8}
$$

$$
\begin{aligned}
\mathcal{H}_M = V_M(\mathbf{r}) &= -\frac{\mu_M}{|\mathbf{r} - \mathbf{r_M}|} + \frac{\mu_M}{r_M^3}\mathbf{r} \cdot \mathbf{r_M} \\
&= -\frac{\mu_M}{r_M} - \frac{\mu_M}{2r_M^3}r^2 + \frac{3}{2}\frac{\mu_M(\mathbf{r} \cdot \mathbf{r}_M)^2}{r_M^5} + O\left(\left(\frac{r}{r_M}\right)^3\right).
\end{aligned} \tag{9}
$$

## 2.2 Average over fast angles: secular Hamiltonian

The secular motion of the body $S$ can be modeled by computing the average of (7) over all canonical angles associated with the fast motions of $S$, the Sun and the Moon. Note that the period of the Sun is only 'semi-fast' (one year, compared to secular periods of $\sim$ 10 yrs for the small body), and more detailed models can consider also the case of 'semi-secular' resonances, i.e., resonances in the case in which the equations of motion (and Hamiltonian) are not averaged with respect to the Sun's mean anomaly (see, for example, Celletti et al. 2017).

Averaging with respect to all fast angles leads to the following, called hereafter, *secular Hamiltonian*, given by the sum of the averaged contributions of the Earth, Sun and Moon:

$$\mathcal{H}^{(sec)} = \mathcal{H}_E^{(av)} + \mathcal{H}_\odot^{(av)} + \mathcal{H}_M^{(av)}. \tag{10}$$

---

[2] In this approximation, with the Moon's and the Sun's elements taken on the ecliptic frame, the Sun's and Moon's longitudes of the nodes do not appear in the Hamiltonian.

The function $\mathcal{H}^{(sec)} = \mathcal{H}^{(sec)}(G, \Theta, \omega, \Omega)$ is a two degrees of freedom Hamiltonian, which can be explicitly computed in terms of Delaunay canonical action-angle variables $G$, $\Theta$ (with conjugated angles $\omega$, $\Omega$), related to the orbital elements by the expressions (see, e.g., Celletti 2010):

$$G = \sqrt{\mu_E a(1 - e^2)}, \quad \Theta = \sqrt{\mu_E a(1 - e^2)} \cos i \ . \tag{11}$$

Since the averaged Hamiltonian does not depend on the mean anomaly $M$ of $S$, the conjugated Delaunay action $L = \sqrt{\mu_E a}$, and hence the semimajor axis $a$, is a constant of motion of the Hamiltonian $\mathcal{H}^{(sec)}$. We set $L = L_*$, or, equivalently, $a = a_*$ when referring to trajectories whose semimajor axis has the reference value $a_*$.

Following a well-known procedure (e.g., Kaula 1962), the various terms in the secular Hamiltonian can be computed as follows: for the geopotential term we have

$$\mathcal{H}_E^{(av)} = \frac{1}{2\pi} \int_0^{2\pi} (\mathcal{H}_{kep} + \mathcal{H}_{J_2}) dM = \mathcal{H}_{kep}^{(av)} + \mathcal{H}_{J_2}^{(av)}, \tag{12}$$

where $\mathcal{H}_{kep} = \mathbf{p}^2/2 + V_{kep}$, $\mathcal{H}_{J_2} = V_{J_2}$, which leads to

$$\mathcal{H}_E^{(av)} = -\frac{\mu_E^2}{2L^2} - J_2 \frac{\mu_E R_E^2}{a_*^3(1 - e^2)^{3/2}} \left( \frac{1}{2} - \frac{3}{4} \sin^2 i \right). \tag{13}$$

We note that this procedure of *scissor averaging* yields a formula for $\mathcal{H}_E^{(av)}$, which is identical to the formula obtained at first order through a Lie canonical transformation, a procedure known as the *Delaunay normalization* (see Palacián 2002 or Lara 2021). However, from a physical point of view, this implies that in all results described below, any reference to the values of the *elements* refers to the ones found after the near-identity transformation, which eliminates from the Hamiltonian all the short-period terms (see discussion in Sect. 5). The same property holds for the averaging of the terms $\mathcal{H}_{\odot}^{(av)}$, $\mathcal{H}_M^{(av)}$, which can be performed by a canonical transformation. Again, to first order this leads formally to the same formula as the one of the scissor averaging integral

$$\mathcal{H}_{\odot}^{(av)} = \frac{1}{4\pi^2} \int_0^{2\pi} \int_0^{2\pi} \left( -\frac{\mu_{\odot}}{r_{\odot}} - \frac{\mu_{\odot}}{2r_{\odot}^3} r^2 + \frac{3}{2} \frac{\mu_{\odot}(\mathbf{r} \cdot \mathbf{r}_{\odot})^2}{r_{\odot}^5} \right) dM dM_{\odot}$$

(and analogously for $\mathcal{H}_M^{(av)}$). However, here too this formula refers to the new elements found after the canonical transformation. In this case, it turns convenient to change the integration variables from $M$ to $u$ (eccentric anomaly of $S$) and from $M_{\odot}$ to $f_{\odot}$ (true anomaly of the Sun). We note that, up to quadrupolar terms, this yields the same result as considering the Moon and Sun in circular, instead of elliptic, orbits (in which case $M_{\odot}$, $M_M$ would be equal to $f_{\odot}$, $f_M$), but replacing each third-body's semimajor axis $a_b$ with the expression $a_b \to a_b(1 - e_b^2)^{1/2}$ (index $b$ standing for Sun or Moon). This replacement accomplishes the first step in the Hamiltonian preparation.

### 2.3 Expansion around reference values ($e_*$, $i_*$)

After performing the above operations, the Hamiltonian $\mathcal{H}^{(sec)}$ becomes a function of the body's action-angle variables $(G, \omega)$, $(\Theta, \Omega)$, while it depends also on the Delaunay action $L$, which however, does not affect the secular dynamics and can be carried on all subsequent expressions as a parameter (equal to $L_*$). We use, alternatively, $a_*$ as the parameter appearing

in the coefficients of all trigonometric terms in $\mathcal{H}^{(sec)}$. Furthermore, it turns convenient to express $\mathcal{H}^{(sec)}$ in terms of *modified Delaunay variables* instead of the original Delaunay variables. Let $\delta L = L - L_*$ with $L_* = \sqrt{\mu_E a_*}$. We employ the modified Delaunay variables $(\delta L, \Gamma, \tilde{\Theta}, \lambda, p, q)$, related to the original Delaunay variables $(L, G, \Theta, M, \omega, \Omega)$ via the latters' dependence on the Keplerian elements $(a, e, i, M, \omega, \Omega)$. We have

$$
\begin{cases}
\delta L = L - L_* = \sqrt{\mu_E a} - \sqrt{\mu_E a_*} \\
\Gamma = L - G = \sqrt{\mu_E a}(1 - \sqrt{1 - e^2}) \\
\tilde{\Theta} = G - \Theta = \sqrt{\mu_E a}\sqrt{1 - e^2}(1 - \cos i)
\end{cases}
\begin{cases}
\lambda = M + \omega + \Omega \\
p = -\omega - \Omega \\
q = -\Omega.
\end{cases}
\tag{14}
$$

Starting now from the Hamiltonian $\mathcal{H}^{(sec)}(\Gamma, \tilde{\Theta}, p, q)$, our goal will be to examine Nekhoroshev stability in a covering of the action space in terms of local neighborhoods around a grid of reference values corresponding to a grid of element values $(a_*, e_*, i_*)$ (see Sect. 3.2). This motivates to introduce the variables $P'$ and $Q'$ defined by

$$
\begin{cases}
P = \Gamma_* - \Gamma, \\
Q = \tilde{\Theta}_* - \tilde{\Theta},
\end{cases}
\tag{15}
$$

where $\Gamma_*$ and $\tilde{\Theta}_*$ are the values corresponding to the orbital elements $(e_*, i_*)$, and compute the Taylor expansion of $\mathcal{H}^{(sec)}$ in powers of the small quantities $(Q, P)$, truncated at a maximum order $N$ (we set $N = 12$). We then arrive at the following truncated secular Hamiltonian model

$$
\mathcal{H}^{(sec,N)}(P, Q, p, q) = \sum_{j=1}^{N} g^{(j)}(P, Q, p, q) \ .
\tag{16}
$$

In the model (16) we have

$$
g^{(1)}(P, Q) = \omega_1 P + \omega_2 Q \ .
\tag{17}
$$

For reasons that will become clear later, for $j \geq 2$ we split each of the functions $g^{(j)}(P, Q, p, q)$ as a sum depending only on the actions and a sum depending also on the angles:

$$
g^{(j)}(P, Q, p, q) = \sum_{\substack{\mathbf{l} \in \mathbb{Z}^2 \\ |\mathbf{l}| = j}} a_{\mathbf{l}}^{(j)} P^{l_1} Q^{l_2} + \sum_{\substack{\mathbf{l}, \mathbf{k} \in \mathbb{Z}^2 \\ |\mathbf{l}| = j-2}} b_{\mathbf{l}, \mathbf{k}}^{(j)} P^{l_1} Q^{l_2} e^{i(k_1 p + k_2 q)} \ .
\tag{18}
$$

This last splitting completes the second step in the Hamiltonian preparation. The explicit expressions of the quantities $\omega_1$, $\omega_2$, $a_{\mathbf{l}}$, $b_{\mathbf{l}, \mathbf{k}}$ for $j = 2$ are given in Appendix 1, in terms of the orbital elements of the satellite, Moon and Sun.

## 2.4 Preliminary normalization

It was already mentioned in Sect. 1 that the presence of the averaged lunisolar terms in (16) implies the existence of a secular equilibrium solution of Hamilton's equation's of motion under the Hamiltonian $\mathcal{H}^{(sec)}$, corresponding to the values $e = 0$, $i = i^{(p)}$ [see Eq. (1)], where $i^{(p)}$ is called the inclination of the *Laplace plane*. It is easy to see that the nonzero value of the inclination of the Laplace plane is reflected into the Hamiltonian $\mathcal{H}^{(sec,N)}$ by the presence of purely trigonometric terms, i.e., terms with $|\mathbf{l}| = 0$. Such terms yield coefficients which are dominant with respect to the remaining terms in the Hamiltonian expansion. Furthermore,

in the splitting of the Hamiltonian as $\mathcal{H} = h_0(\mathbf{I}) + h_1(\mathbf{I}, \mathbf{u})$, where $(\mathbf{I}, \mathbf{u})$ are action-angle variables, as required for the implementation of the Nekhoroshev theorem (see next section), the above terms generate terms with a dominant coefficient largely affecting the size of the perturbation $h_1(\mathbf{I}, \mathbf{u})$. In the present subsection, we implement a procedure for controlling the size of the terms (16) of the expansion, so that we obtain a Hamiltonian satisfying the norm bounds required for the implementation of the Nekhoroshev theorem.

More specifically, the aim of the normalization algorithm described below is to remove, up a certain order $N_{norm}$ with respect to the expansion (16), the angle-dependent terms which are constant or linear in the actions: this leads to a Hamiltonian $\mathcal{H}^{(N_{norm})}$, in which the norm of the angle-dependent part decreases at least quadratically with the size of the domain $A_{r_0}$ in which local action variables are defined.

The normalization procedure relies on the use of *Lie series*. In every normalization step, the transformed Hamiltonian is given by

$$\mathcal{H}^{(new)} = \exp^{(N)}(\mathcal{L}_\chi)\mathcal{H}^{(old)}, \tag{19}$$

where $\mathcal{L}_\chi f = \{f, \chi\}$ ($\{\cdot, \cdot\}$ denotes the *Poisson bracket*) and $\exp^{(N)}(\mathcal{L}_\chi)$ is defined by

$$\exp^{(N)}(\mathcal{L}_\chi)f = \sum_{s=0}^{N} \frac{1}{s!}\mathcal{L}_\chi^s f. \tag{20}$$

To illustrate the procedure, rename the initial Hamiltonian (16) as $\mathcal{H}^{(0)}$ (where superscripts denote how many normalization steps were performed). Then:

$$\mathcal{H}^{(0)}(P, Q, p, q) = \sum_{j=1}^{N} g^{(j,0)}(P, Q, p, q), \tag{21}$$

where

$$g^{(1,0)}(P, Q) = \omega_1 P + \omega_2 Q$$
$$g^{(j,0)}(P, Q, p, q) = \sum_{\substack{\mathbf{l} \in \mathbb{Z}^2 \\ |\mathbf{l}|=j}} a_{\mathbf{l}}^{(j,0)} P^{l_1} Q^{l_2} + \sum_{\substack{\mathbf{l},\mathbf{k} \in \mathbb{Z}^2 \\ |\mathbf{l}|=j-2}} b_{\mathbf{l},\mathbf{k}}^{(j,0)} P^{l_1} Q^{l_2} e^{i(k_1 p + k_2 q)}, \quad j \geq 2. \tag{22}$$

The second term of the sum (21) takes the form

$$g^{(2,0)}(P, Q, p, q) = \sum_{\substack{\mathbf{l} \in \mathbb{Z}^2 \\ |\mathbf{l}|=2}} a_{\mathbf{l}}^{(2,0)} P^{l_1} Q^{l_2} + \sum_{\mathbf{k} \in \mathbb{Z}^2} b_{\mathbf{0},\mathbf{k}}^{(2,0)} e^{i(k_1 p + k_2 q)}. \tag{23}$$

The generating function $\chi^{(1)}$ eliminating the above terms has the form

$$\chi^{(1)}(P, Q, p, q) = \sum_{\mathbf{l},\mathbf{k} \in \mathbb{Z}^2} x_{\mathbf{l},\mathbf{k}}^{(1)} P^{l_1} Q^{l_2} e^{i(k_1 p + k_2 q)}, \tag{24}$$

where the coefficients $x_{\mathbf{l},\mathbf{k}}^{(1)}$ are obtained as the solution of the homological equation

$$\{\omega_1 P + \omega_2 Q, \chi^{(1)}\} = -\sum_{\mathbf{k} \in \mathbb{Z}^2} b_{\mathbf{0},\mathbf{k}}^{(2,0)} e^{i(k_1 p + k_2 q)}, \tag{25}$$

namely

$$\chi^{(1)}(p, q) = -\sum_{\mathbf{k} \in \mathbb{Z}^2} \frac{b_{\mathbf{0},\mathbf{k}}^{(2,0)}}{i(\omega_1 k_1 + \omega_2 k_2)} e^{i(k_1 p + k_2 q)}. \tag{26}$$

The normalized Hamiltonian after the first step can be written as

$$\mathcal{H}^{(1)}(P, Q, p, q) = \omega_1 P + \omega_2 Q + Z^{(2,1)}(P, Q, p, q) + \sum_{j=3}^{N} g^{(j,1)}(P, Q, p, q), \quad (27)$$

where

$$Z^{(2,1)} = g^{(2,0)} + \mathcal{L}_{\chi^{(1)}}(\omega_1 P + \omega_2 Q) = \sum_{\substack{\mathbf{l} \in \mathbb{Z}^2 \\ |\mathbf{l}|=2}} a_{\mathbf{l}}^{(2,0)} P^{l_1} Q^{l_2} \quad (28)$$

and

$$g^{(j,1)} = \sum_{s=0}^{j-1} \frac{1}{s!} \mathcal{L}_{\chi^{(1)}}^{s} g^{(j-s,1)}. \quad (29)$$

In general, since the generating function $\chi^{(1)}$ is constant in the actions, one can see that, if $f(P, Q, p, q)$ has polynomial order $\ell$ in the actions, then the order in the actions of the transformed function $\mathcal{L}_{\chi^{(1)}} f$ is $\ell - 1$. This means that all terms in $\mathcal{H}^{(1)}$ can be labeled through their polynomial orders in the actions: choosing the expansion order $N$ to be odd and distinguishing the indices $j$ with respect to their parity, we have, for $n = 1, \ldots, (N-1)/2$:

$$g^{(2n,1)}(P, Q, p, q) = \sum_{\substack{\mathbf{l} \in \mathbb{Z}^2 \\ |\mathbf{l}|=2n}} a_{\mathbf{l}}^{(2n,1)} P^{l_1} Q^{l_2} + \sum_{s=0}^{n-1} \sum_{\substack{\mathbf{l}, \mathbf{k} \in \mathbb{Z}^2 \\ |\mathbf{l}|=2s}} b_{\mathbf{l}, \mathbf{k}}^{(2n,1)} P^{l_1} Q^{l_2} e^{i(k_1 p + k_2 q)} \quad (n \geq 2),$$

$$g^{(2n+1,1)}(P, Q, p, q) = \sum_{\substack{\mathbf{l} \in \mathbb{Z}^2 \\ |\mathbf{l}|=2n+1}} a_{\mathbf{l}}^{(2n+1,1)} P^{l_1} Q^{l_2} + \sum_{s=0}^{n-1} \sum_{\substack{\mathbf{l}, \mathbf{k} \in \mathbb{Z}^2 \\ |\mathbf{l}|=2s+1}} b_{\mathbf{l}, \mathbf{k}}^{(2n+1,1)} P^{l_1} Q^{l_2} e^{i(k_1 p + k_2 q)}.$$

$$(30)$$

After the classical normalization step, the function $Z^{(2,1)}(P, Q, p, q)$ does not contain angle-dependent terms which are constant or linear in the actions.

The second step focusses on the manipulation of the term

$$g^{(3,1)}(P, Q, p, q) = \sum_{\substack{\mathbf{l} \in \mathbb{Z}^2 \\ |\mathbf{l}|=3}} a_{\mathbf{l}, \mathbf{k}}^{(3,1)} P^{l_1} Q^{l_2} + \sum_{\substack{\mathbf{l}, \mathbf{k} \in \mathbb{Z}^2 \\ |\mathbf{l}|=1}} b_{\mathbf{l}, \mathbf{k}}^{(3,1)} P^{l_1} Q^{l_2} e^{i(k_1 p + k_2 q)}. \quad (31)$$

Precisely, the second normalization step aims to remove the second sum in $g^{(3,1)}$ which is angle-dependent and linear in the actions. The generating function $\chi^{(2)}$, given by (24) with a suitable change in the upper indexes, must satisfy the normal form equations

$$\{\omega_1 P + \omega_2 Q, \chi^{(2)}\} = - \sum_{\substack{\mathbf{l}, \mathbf{k} \in \mathbb{Z}^2 \\ |\mathbf{l}|=1}} b_{\mathbf{l}, \mathbf{k}}^{(3,1)} P^{l_1} Q^{l_2} e^{i(k_1 p + k_2 q)}, \quad (32)$$

which gives

$$\chi^{(2)}(P, Q, p, q) = - \sum_{\substack{\mathbf{l}, \mathbf{k} \in \mathbb{Z}^2 \\ |\mathbf{l}|=1}} \frac{b_{\mathbf{l}, \mathbf{k}}^{(3,1)}}{i(\omega_1 k_1 + \omega_2 k_2)} P^{l_1} Q^{l_2} e^{i(k_2 p + k_2 q)}.$$

As a result, the generating function $\chi^{(2)}$ is linear in the actions, so that the operator $\mathcal{L}_{\chi^{(2)}} f$ preserves the polynomial degree in the actions of any generic function $f(P, Q, p, q)$.

The second-order transformed Hamiltonian $\mathcal{H}^{(2)}$ can be written as

$$\mathcal{H}^{(2)}(P, Q, p, q) = \omega_1 P + \omega_2 Q + \sum_{j=2}^{3} Z^{(j,2)}(P, Q) + \sum_{j=4}^{N} g^{(j,2)}(P, Q, p, q), \quad (33)$$

where, noticing that $g^{(0,2)} \equiv 0$, one obtains

$$Z^{(2,2)} = \sum_{\substack{\mathbf{l} \in \mathbb{Z}^2 \\ |\mathbf{l}|=2}} a_{\mathbf{l}}^{(2,2)} P^{l_1} Q^{l_2}, \quad Z^{(3,2)} = \sum_{\substack{\mathbf{l} \in \mathbb{Z}^2 \\ |\mathbf{l}|=3}} a_{\mathbf{l}}^{(3,2)} P^{l_1} Q^{l_2}, \quad g^{(j,2)} = \sum_{s=0}^{\lfloor \frac{j}{2} \rfloor} \frac{1}{s!} \mathcal{L}^s g^{(j-2s,2)}.$$

$$(34)$$

Taking into account the parities of the indexes $j$, one can obtain also for $g^{(j,2)}$ the analogous of (30).

We can now give the explicit formulas for the normalization steps for $r > 2$.

- The $r-$th normalization step allows one to transform the Hamiltonian

$$\mathcal{H}^{(r-1)}(P, Q, p, q) = \omega_1 P + \omega_2 Q + \sum_{j=2}^{r-1} Z^{(j,r-1)}(P, Q, p, q)$$

$$+ \sum_{j=r}^{N} g^{(j,r-1)}(P, Q, p, q) \quad (35)$$

into

$$\mathcal{H}^{(r)}(P, Q, p, q) = \omega_1 P + \omega_2 Q + \sum_{j=2}^{r} Z^{(j,r)}(P, Q, p, q)$$

$$+ \sum_{j=r+1}^{N} g^{(j,r)}(P, Q, p, q), \quad (36)$$

with

$$Z^{(2,r)} = \sum_{\substack{\mathbf{l} \in \mathbb{Z}^2 \\ |\mathbf{l}|=2}} a_{\mathbf{l}}^{(2,r)} P^{l_1} Q^{l_2}, \quad Z^{(3,r)} = \sum_{\substack{\mathbf{l} \in \mathbb{Z}^2 \\ |\mathbf{l}|=3}} a_{\mathbf{l}}^{(3,r)} P^{l_1} Q^{l_2},$$

$$Z^{(j>3,r)} = \sum_{\substack{\mathbf{l} \in \mathbb{Z}^2 \\ |\mathbf{l}|=j}} a_{\mathbf{l}}^{(j,r)} P^{l_1} Q^{l_2} + \sum_{s=2}^{j-2} \sum_{\substack{\mathbf{l},\mathbf{k} \in \mathbb{Z}^2 \\ |\mathbf{l}|=s}} b_{\mathbf{l},\mathbf{k}}^{(j,r)} P^{l_1} Q^{l_2} e^{i(k_1 p + k_2 q)},$$

$$g^{(j,r)} = \sum_{\substack{\mathbf{l} \in \mathbb{Z}^2 \\ |\mathbf{l}|=j}} a_{\mathbf{l}}^{(j,r)} P^{l_1} Q^{l_2} + \sum_{s=0}^{j-2} \sum_{\substack{\mathbf{l},\mathbf{k} \in \mathbb{Z}^2 \\ |\mathbf{l}|=s}} b_{\mathbf{l},\mathbf{k}}^{(j,r)} P^{l_1} Q^{l_2} e^{i(k_1 p + k_2 q)}. \quad (37)$$

By the above parity rules, which apply also for $r > 3$, both $Z^{(j,i)}$ and $g^{(j,i)}$ contain only the terms with $s$ even if $j$ is even and $s$ odd if $j$ is odd. Notice that, for $j > 3$, $Z^{(j,i)}$ can contain also angle-dependent terms, which are at least quadratic in the actions.

- The $r$-th order generating function can be expressed as

$$\chi^{(r)}(P, Q, p, q) = - \sum_{\substack{\mathbf{l}, \mathbf{k} \in \mathbb{Z}^2 \\ |\mathbf{l}|=0,1}} \frac{b_{\mathbf{l},\mathbf{k}}^{(r+1,r-1)}}{i(\omega_1 k_1 + \omega_2 k_2)} P^{l_1} Q^{l_2} e^{i(k_1 p + k_2 q)}, \tag{38}$$

  which contains only purely trigonometric terms (independent on the actions) if $r$ is odd and only terms linear in the actions if $r$ is even.
- After $N_{norm}$ normalization steps, the final Hamiltonian is given by

$$\mathcal{H}^{(N_{norm})}(P, Q, p, q) = \omega_1 P + \omega_2 Q + \sum_{j=2}^{N_{norm}} Z^{(j,N_{norm})}(P, Q, p, q)$$

$$+ \sum_{j=N_{norm}+1}^{N} g^{(j,N_{norm})}(P, Q, p, q). \tag{39}$$

From (37), it is clear that the functions $g^{(j,\ell)}$ might contain terms which are angle-dependent and constant or linear in the actions. As we will see later, the series are convergent in particular domains of the parameters. In that case, the normalization procedure succeeds to reduce the magnitude of all the terms in the perturbation to a size sufficiently small for the application of the Nekhoroshev theorem.

It is also important to observe that particular angle combinations in the angle-dependent part of the Hamiltonians can produce, if $r$ is odd, constant terms both in actions and angles, which do not affect the dynamics; however, when $r$ is even, the same combinations can produce terms which do not depend on the angles, but are linear in the actions. These terms represent a perturbation on the frequencies, which can have important effects on the applicability of Nekhoroshev theorem.

From the definition of the $r-$th order generating function (38), one can observe that the convergence of the normalization algorithm depends heavily on the presence of *resonances*, which produce small divisors of the type $\omega_1 k_1^{(res)} + \omega_2 k_2^{(res)} \approx 0$ for suitable integers $k_1^{(res)}$, $k_2^{(res)}$. Section 4.2 provides numerical examples of how the presence of resonances can affect the convergence of the normalization procedure, along with effects on the variation of the initial frequencies.

## 3 Nekhoroshev stability estimates

In this Section, we recall the version of the Nekhoroshev theorem developed in Pöschel (1993) for frequencies satisfying a non-resonance condition (see Sect. 3.1). Based on this theorem, we developed an algorithm computing all quantities needed in order to check whether the necessary conditions for the holding of the theorem are fulfilled in the case of the Hamiltonian (39). The algorithm is presented in Sect. 3.2.

### 3.1 Theorem on exponential stability

Let us consider an $n-$dimensional quasi-integrable Hamiltonian of the form

$$\mathcal{H}(\mathbf{I}, \mathbf{u}) = h(\mathbf{I}) + f_\epsilon(\mathbf{I}, \mathbf{u}),$$

with $h$ called the integrable part and $f_\epsilon$ the perturbing function, depending on a small real parameter $\epsilon > 0$. The Hamiltonian $\mathcal{H}$ is assumed real analytic in the domain $(\mathbf{I}, \mathbf{u}) \in A \times \mathbb{T}^n$ with $A \subseteq \mathbb{R}^n$ open and bounded. Besides, we assume that $\mathcal{H}$ can be extended analytically to the set $D_{r_0, s_0}$ defined as

$$D_{r_0, s_0} = A_{r_0} \times \mathbb{T}^n_{s_0}, \tag{40}$$

where for $r_0, s_0 > 0$:

$$A_{r_0} = \{\mathbf{I} \in \mathbb{C}^n : dist(\mathbf{I}, A) < r_0\} \tag{41}$$

and

$$\mathbb{T}^n_{s_0} = \{\mathbf{u} \in \mathbb{C}^n : Re(u_j) \in \mathbb{T}, \ \max_{j=1,\dots,n} |Im(u_j)| < s_0\}.$$

Finally, we assume that there exists a positive constant $M$ such that

$$\sup_{\mathbf{I} \in A_{r_0}} \|\mathcal{Q}(\mathbf{I})\|_o \leq M,$$

where $\mathcal{Q}$ denotes the Hessian matrix associated with $h$ and $\| \cdot \|_o$ denotes the operator norm induced by the Euclidean norm on $\mathbb{R}^n$.

For any analytic function

$$g(\mathbf{I}, \mathbf{u}) = \sum_{\mathbf{k} \in \mathbb{Z}^n} g_{\mathbf{k}}(\mathbf{I}) e^{i\mathbf{k} \cdot \mathbf{u}},$$

in $D_{r_0, s_0}$, we define its Cauchy norm as

$$|g|_{A, r_0, s_0} = \sup_{\mathbf{I} \in A_{r_0}} \sum_{\mathbf{k} \in \mathbb{Z}^n} |g_{\mathbf{k}}(\mathbf{I})| e^{|\mathbf{k}| s_0}, \tag{42}$$

where $|\mathbf{k}|$ is the $\ell^1$-norm of $\mathbf{k} \in \mathbb{Z}^n$. Finally, let $\epsilon$ be such that

$$|f_\epsilon|_{A, r_0, s_0} \leq \epsilon. \tag{43}$$

The following Theorem provides a bound on the action variables for exponentially long times; we refer to Pöschel (1993) for the proof and further extensions. First, we need the following definition.

**Definition 1** A set $D \subseteq A$ is said to be a completely $\alpha, K$-non-resonant domain in $A$, if for every $\mathbf{k} \in \mathbb{Z}^n \backslash \{\mathbf{0}\}$, $|\mathbf{k}| \leq K$, and for every $\mathbf{I} \in D$

$$|\mathbf{k} \cdot \boldsymbol{\omega}(\mathbf{I})| \geq \alpha > 0, \tag{44}$$

where $\boldsymbol{\omega}(\mathbf{I}) = \partial_{\mathbf{I}} h(\mathbf{I})$.

**Theorem 2** (Pöschel (1993)) *Let $D \subseteq A$ be a completely $\alpha, K$-non-resonant domain. Let $a, b > 0$ such that $\frac{1}{a} + \frac{1}{b} = 1$. Let $\epsilon$ be as in (43) for some $r_0, s_0 > 0$. If the following inequalities are satisfied:*

$$\epsilon \leq \frac{1}{2^7 b} \frac{\alpha r}{K} = \epsilon^*, \quad r \leq \min\left(\frac{\alpha}{aMK}, r_0\right), \tag{45}$$

*then, denoting by $\| \cdot \|$ the Euclidean norm in A, one has*

$$\|\mathbf{I}(t) - \mathbf{I}_0\| \leq r \quad for \quad |t| \leq \frac{s_0 r}{5\epsilon} e^{K s_0/6} \tag{46}$$

*for every orbit of the perturbed system with initial position $(\mathbf{I}_0, \mathbf{u}_0)$ in $D \times \mathbb{T}^n$.*

### 3.2 Algorithm for the application of the theorem

To apply Theorem 2 to the final Hamiltonian $\mathcal{H}^{(N_{norm})}$ defined in (39), one has to compute all the quantities involved in the Theorem. This procedure gives rise to an explicit constructive algorithm to give stability estimates for every pair of reference values $(e_*, i_*)$ in the uniform grid $[0, 0.5] \times [0, 89.5°]$ with step-size equal to 0.1 in eccentricity and $0.5°$ in inclination. Notice that the upper value of the grid in inclination is equal to $89.5°$ to avoid singularities.

First, we need to determine the greatest integer $\bar{K}$, to which we refer as the *cut-off value*, such that conditions (45) hold. From the definition of $\alpha$ in (44) and $\epsilon^*$ in (45), it is clear that $\epsilon^*$ decreases as $K$ increases; then, provided that condition (45) holds for $K = 1$, the maximal value $\bar{K}$ exists. On the other hand, if (45) does not hold for $K = 1$, it continues to remain false for all $K > 1$.

From a computational point of view, the procedure is composed by the following steps, (S1),..., (S8), performed for every pair $(e_*, i_*)$ in the grid defined above; by trial and error, we fix the values of $r_0$, $s_0$, $a$, $b$. Their choice is arbitrary and can be tuned so to satisfy the conditions of the Theorem and to optimize the final estimates.

(S1) Taylor expansion up to order $N = 12$ in the expansion (16) around the actions $(P_*, Q_*)$, corresponding to the Keplerian elements $(e_*, i_*)$ with the precise values inserted after the symbolic expansion;

(S2) normalization up to order $N_{norm} = 6$, following the procedure described in Sect. 2.4, which leads to compute the normalized Hamiltonian $\mathcal{H}^{(N_{norm})}$;

(S3) splitting of the Hamiltonian $\mathcal{H}^{(N_{norm})}$ in the unperturbed part $h_0(P, Q)$, containing the terms of $\mathcal{H}^{(N_{norm})}$ which depend only on the actions, and the perturbing part $h_1(P, Q, p, q) = \mathcal{H}^{(N_{norm})}(P, Q, p, q) - h_0(P, Q)$; computation[3] of $\boldsymbol{\omega} = (\omega_1, \omega_2)$, with $\omega_1$ and $\omega_2$ coefficients respectively of $P$ and $Q$ in $h_0$;

(S4) definition of the real and complexified domains in the actions as in (40) and computation of the quantity

$$M = \sup_{(P,Q) \in A_{r_0}} ||\mathcal{Q}(P, Q)||_o \tag{47}$$

in particular, we define $A = [P_* - dP^{(max)}, P_* + dP^{(max)}] \times [Q_* - dQ^{(max)}, Q_* + dQ^{(max)}]$ with $dP^{(max)} = dQ^{(max)} = 0.1$; we select $r_0 = s_0 = 0.1$ and, following (Pöschel 1993), we take $a = 9/8$ and $b = 9$;

(S5) for every $K = 1, \ldots, 50$, computation of the quantities

$$\alpha_K = \min_{|\mathbf{l}| \le K} \{\boldsymbol{\omega} \cdot \mathbf{l}\}, \qquad r_K = \min\left\{\frac{\alpha_K}{aMK}, r_0\right\}, \qquad \epsilon_K^* = \frac{1}{2^7 b}\frac{\alpha_K r_K}{K} \tag{48}$$

(S6) defining $\epsilon = |h_1|_{A, r_0, s_0}$, check of the condition $\epsilon \le \epsilon_K^*$ for every $K = 1, \ldots, 50$;

(S7) if $\epsilon \le \epsilon_1^*$, computation of $\bar{K}$, namely the greatest $K$ such that $\epsilon \le \epsilon_K^*$, and of the corresponding stability time

$$t = \frac{s_0 r_{\bar{K}}}{5\epsilon} e^{\bar{K} s_0/6} \tag{49}$$

(S8) if $\epsilon > \epsilon_1^*$, the conditions for the application of Theorem 2 are not satisfied. In this case, we impose $\bar{K} = 0$.

---

[3] With an abuse of notation, we continue to define the new frequencies, which could be modified by the normalization, with the symbols $\omega_1$ and $\omega_2$. When, in Sect. 4.2, it will be required to distinguish between the initial and the final frequencies, the latter will be denoted by $\tilde{\omega}_1$ and $\tilde{\omega}_2$.

**Table 2** Inclination-dependent resonances which affect the stability in the lunisolar model. The coefficients $\alpha$ and $\beta$ are such that $\alpha \dot{p} + \beta \dot{q} = 0$

| $\alpha$ | $\beta$ | $i(deg)$ | $\alpha$ | $\beta$ | $i(deg)$ | $\alpha$ | $\beta$ | $i(deg)$ | $\alpha$ | $\beta$ | $i(deg)$ |
|---|---|---|---|---|---|---|---|---|---|---|---|
| 1 | 0 | 46.37 | 0 | 1 | 90 | 1 | 1 | 0 | 1 | $-1$ | 63.4351 |
| 2 | 1 | 33.0156 | $-1$ | 2 | 73.1484 | $-2$ | 1 | 56.0646 | $-2$ | 3 | 69.007 |
| $-4$ | 3 | 60.0001 | $-4$ | 1 | 51.5596 | $-1$ | 3 | 78.4633 | $-4$ | 5 | 66.422 |

We remark that the order of the Taylor expansion $N = 12$, the order of normalization $N_{norm} = 6$, the iteration of $K$ up to 50 are set on the basis of having a reasonable computational execution time on standard laptops.

## 4 Results

In this Section, we present the results of the application of Theorem 2 to the Hamiltonian model described in Sect. 2. This allows us to derive stability estimates as well as to discuss the convergence of the normalization procedure.

### 4.1 Stability estimates

We apply the algorithm of Sect. 3.2 to prove the Nekhoroshev stability for satellites with semimajor axes between 11 000 km and 19 000 km under the model presented in Sect. 2. The results exposed below highlight the strong dependence of the stability conditions on the precise values of the elements $(e, i)$. Of crucial role in this dependence is the location of the 'inclination-dependent' resonances (see Sect. 1). These satisfy a condition of the form $\alpha \dot{p} + \beta \dot{q} = 0$ for some coefficients $\alpha$, $\beta \in \mathbb{Z}$.

Table 2 shows the values of the inclinations corresponding to each pair of coefficients $(\alpha, \beta)$. We find that these resonances determine regions where Theorem 2 cannot be applied. This can be exemplified with the help of Fig. 1, showing (in blue) the region where the algorithm of Sect. 3.2 returns that the necessary conditions of Theorem 2 hold true. The algorithm provides an answer as a function of the chosen reference values $i_*$ and $e_*$ (for a fixed $a_*$). We take the values of $i_*$ in a grid by steps of 0.5° in the interval $0 \leq i_* \leq 89.5°$, and of $e_*$ in a grid by steps of 0.1 in the interval $0 \leq e_* \leq 0.5$. Figure 2 shows the Nekhoroshev stability times computed at every grid point $(e_*, i_*)$ where the algorithm returns a positive answer for the holding of the necessary conditions of the theorem.

It is evident from Fig. 1 that increasing the distance from the Earth's center causes a shrinking of the size of the domains of Nekhoroshev stability, as well as a fast decrease in the corresponding computed stability times. From the physical point of view, this tendency is evident and can be explained on the basis of the simple remark that the averaged Hamiltonian $\mathcal{H}_{kep} + \mathcal{H}_{J_2}$ without third-body perturbations is integrable (the averaged Hamiltonian has no dependence on the Delaunay angles). Since the overall relative size of third-body perturbations increases with the altitude, these perturbations affect the stability more as $a_*$ increases. At a formal level the effect of the semimajor axis on the estimates can be identified by an analysis of the convergence of the preliminary normalization algorithm (see Sect. 4.2 below).

On the other hand, also evident from Fig. 1 is the strong role of resonances in affecting the stability properties of the system: in fact, around everyone of the resonances listed in
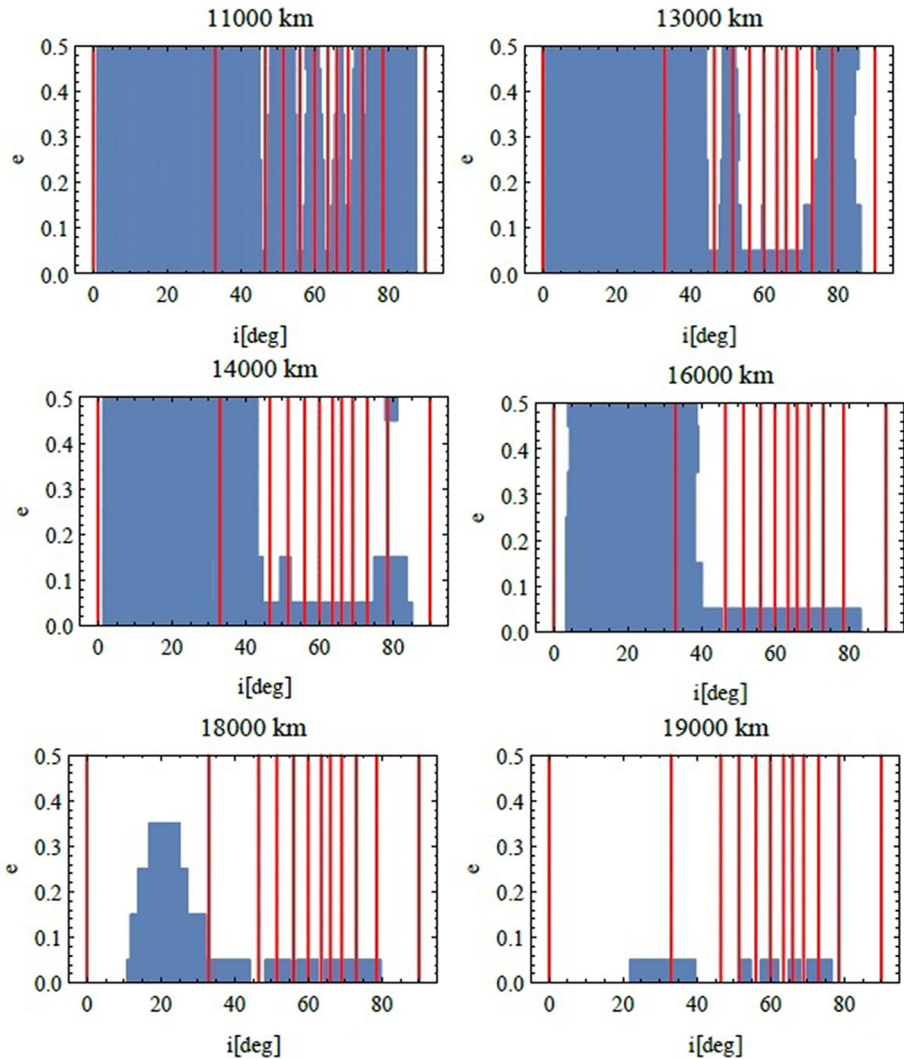
**Fig. 1** Domains of applicability of Theorem 2 for different values of the altitude. The blue regions represent the values of $(i_*, e_*)$ for which the Theorem can be applied, while the red lines define the values of the inclination which are associated with the most important resonances in the considered regions (see Table 2)

Table 2 we observe, in the figure, the formation of a white zone, which indicates values $(e_*, i_*)$ excluded from the Nekhoroshev stability as detected by our algorithm. As a general comment, the presence of the resonances acts at two different stages of the computation:

(i) it can affect the convergence of the classical normalization, producing an increase in the size of the perturbing function and a consequent failure of conditions (45);

(ii) near the low-order resonant values of the inclination, the quantity $\alpha_K$ (see (48)) can be extremely small, even for low values of $K$. As a consequence, in the proximity of a resonance, the corresponding value of the quantity $\epsilon_K^*$ might not be small enough to satisfy (45).
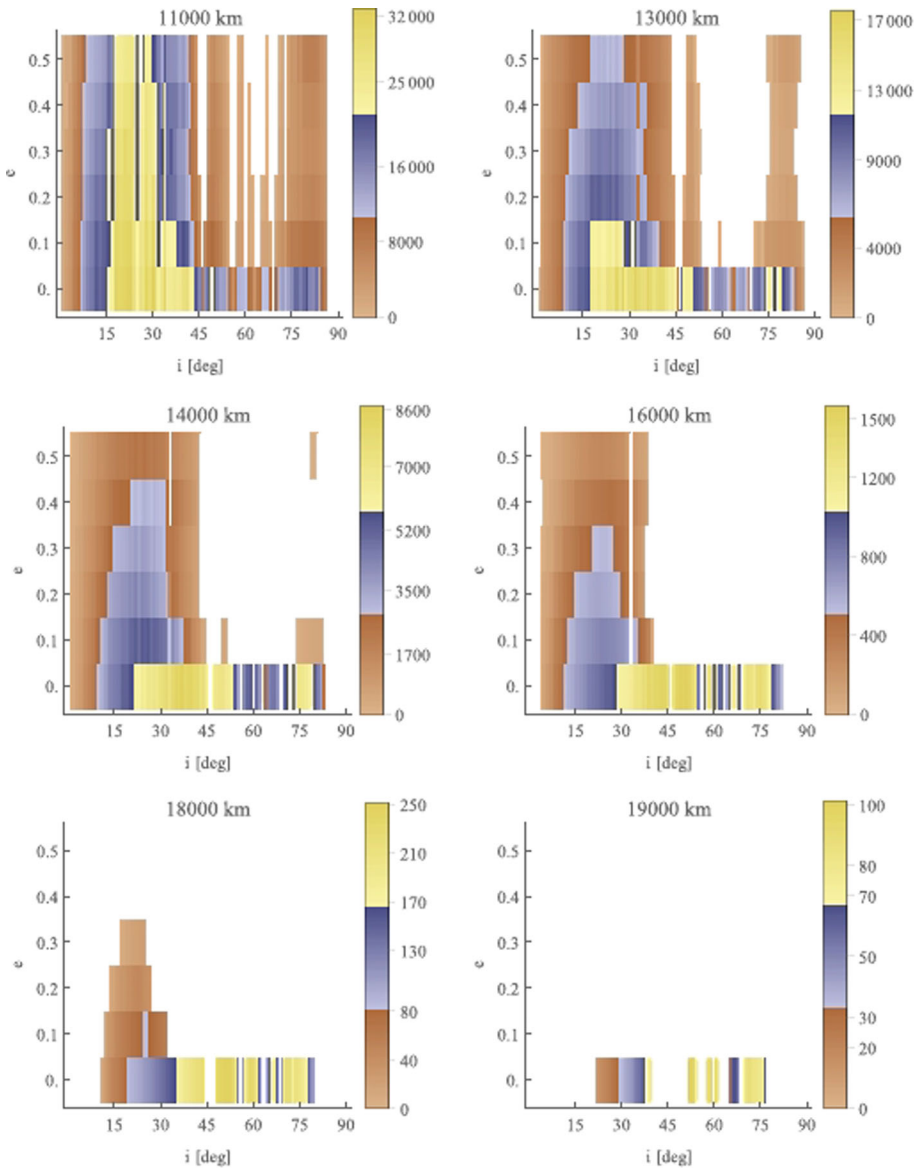
**Fig. 2** Stability time (in years) computed for the values of $(i_*, e_*)$ in the domain of applicability of Theorem 2

At any rate, we stress that Theorem 2 used in the present work holds only for non-resonant domains in the phase space; therefore, by definition it cannot be used to probe the Nekhoroshev stability very close to resonances. We defer to a future study the question of the precise investigation of the conditions for Nekhoroshev stability inside resonances, by implementing a resonant form of the theorem, as first suggested in Nekhoroshev (1977).
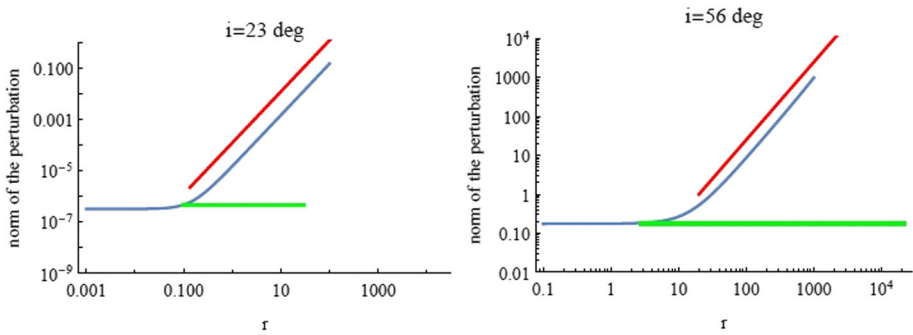
**Fig. 3** Blue: plot in $LogLog$ scale of $|f_\epsilon|_{A,r,s_0}$ for $a = 13\,000$ km, $e_* = 0.2$, and $i_* = 23°$ (left) and $i_* = 56°$ (right). For the computations, we selected $A = [P_* - r, P_* + r] \times [Q_* - r, Q_* + r]$, $r_0 = r$, $s_0 = 0.1$. The slope of the plot for high $r$ is compared with that of a line with slope 2 (red); the value at the plateau (denoted with a green line) is compared with the value of the norm of the purely trigonometric part of $f_\epsilon$ with $s_0 = 0.1$

## 4.2 Convergence of the preliminary normalization

As pointed out in Sect. 2.4, the aim of the preliminary normalization is to allow to control the norm of the perturbing function $|f_\epsilon|_{A,r_0,s_0}$ by reducing the size of the complexified action domain $A_{r_0}$ (see (41)). In particular, the consequence of the removal of angle-dependent terms which are constant or linear in the actions is that, within certain values of the size of the domain $A_{r_0}$, the norm of the perturbation decreases quadratically with the actions.

Figure 3 shows the behavior of $|f_\epsilon|_{A,r,s_0}$ for $a = 13\,000$ km, $e_* = 0.2$ and two selected values of $i_*$, as a function of the size of the action in the complexified domain $A_r$ (the domain $A$ is set to be a rectangle of width $2r$ around the central values $P_*$ and $Q_*$). As expected, the value of $|f_\epsilon|_{A,r,s_0}$ decreases quadratically with $r$, until it reaches a plateau, whose value is the norm of the terms of $f_\epsilon$ which do not depend on the actions.

As already mentioned in Sect. 4.1, the convergence of the normalization presented in Sect. 2.4 for $\mathcal{H}^{(sec)}$ is crucial to control the size of the perturbing function $h_1$; such value plays a fundamental role in Theorem 2. A first study of the effect of the chosen value of the semimajor axis on the convergence can be performed by considering a simpler model to which a normalization procedure similar to the one implemented in Sect. 2.4 can be performed. The model is defined by the Hamiltonian

$$\tilde{\mathcal{H}}^{(in)}(P, Q, p, q) = \omega_1 P + \omega_2 Q + \frac{c_2}{2} Q^2 + f_1 \cos q, \tag{50}$$

where the frequencies $\omega_1, \omega_2$ and the coefficient $c_2$ depend essentially only on the $J_2$ averaged Hamiltonian, while the coefficient $f_1$ depends on the lunar and solar third-body perturbation potentials, and it is proportional to the sinus of the inclination $i_0$ of the ecliptic. We will examine the effect of performing the preliminary normalization algorithm on the Hamiltonian $\tilde{\mathcal{H}}^{(in)}$ so as to remove purely trigonometric terms. After $N_{norm}$ normalization steps, the Hamiltonian takes the form:

$$\tilde{\mathcal{H}}^{(fin)} = \omega_1 P + \omega_2 Q + \frac{c_2}{2} Q^2 + \sum_{i=1}^{N_{norm}} Z_i(P, Q, q) + \sum_{i=N_{norm}+1}^{\infty} R_i(P, Q, q), \tag{51}$$

where the normalized parts $Z_i(P, Q, q)$ do not contain terms which depend only on the angle $q$ (as well as linear terms in the actions multiplied by trigonometric terms). By an

explicit computation of the Poisson brackets involved in the normalization, we readily find that $R_{N_{norm}+1}$ contains trigonometric terms with coefficients proportional to the quantity

$$2^b f_1 \left( \frac{c_2 f_1}{4\omega_2^2} \right)^{N_{norm}} , \tag{52}$$

where $b = 1, 2, 3$ depends on the value of $N_{norm}$. The convergence of the remainder through the steps of the normalization algorithm depends, then, on the value of the ratio $c_2 f_1/4\omega_2^2$; in particular, when this quantity is greater than 1, the normalization does not converge. Neglecting the lunar and solar contributions in $\omega_1$, $\omega_2$ and $c_2$, the coefficient $c_2 f_1/4\omega_2^2$ can be expressed in terms of the orbital elements of debris, Sun and Moon as

$$\frac{c_2 f_1}{4\omega_2^2} = \frac{1}{32} \frac{\sin 2i_0}{R_E^2 \mu_E J_2} \left( \frac{\mu_M}{(a_M(1 - e_M))^3} \right.$$
$$\left. + \frac{\mu_\odot}{(a_\odot(1 - e_\odot))^3} \right) a^5 (2 + 3e_*^2)(1 - e_*^2)^{3/2} \tan i_* . \tag{53}$$

As a consequence, it is clear that its size strongly depends on $a$ and $i_*$: it grows sharply when $a$ increases and when $i_*$ approaches $90°$.

On the other hand, the coefficient $f_1$ is proportional to $\sin 2i_0$, that is, proportional to the (nonzero) inclination $i^{(p)}$ of the Laplace plane (see Eqs. (1) and (2)). Hence, the presence in the secular Hamiltonian of purely trigonometric terms is a manifestation of the presence in the model of a Laplace plane. Since $i^{(p)}$ increases with $a$ and $f_1$ increases both with $i^{(p)}$ and $i_*$, this gives a first explanation of the loss of stability of the model as $a$ and $i_*$ increase.

As already mentioned in Sect. 4.1, the other important factor influencing the size of the remainder across the preliminary normalization process is the effect of resonances, which, due to Eq. (38), leads to the appearance, in the series terms, of small divisors. Of particular importance are the small divisors appearing in the series' purely trigonometric terms, whose size cannot be controlled by altering the size of the domain in the actions $A_{r_0}$.

Figure 4 shows the behavior of the norm of the purely trigonometric part of the perturbation $h_1$ (with the notation (S3) of Sect. 3.2) as a function of the inclination for four different values of $a$ and two different values of $e$. As one can see, the size of the trigonometric part reaches its peaks in correspondence with the resonant values of the inclination, as expected. We also notice that the number of resonances involved in the growth of the size of the trigonometric part increases with $a$ and $e$.

As explained in Sect. 2.4, the normalization algorithm used in this work does not perform a re-tuning of the frequencies for every normalization step. This fact has important effects on the applicability of Theorem 2: when the normalization converges, the change between the original and the new frequencies is negligible with respect to their magnitude; on the other hand, when it does not converge, a large variation in the value of the frequencies occurs, with important consequences on the computation of $\alpha_K$ and, therefore, of the quantities involved in Theorem 2.

As an example, Fig. 5 shows the variations of the frequencies as a function of the inclination for $a = 13\,000$ km and $e_* = 0.2$. Comparing Figs. 4 and 5, it is clear that the resonances which affect the growth in size of the purely trigonometric part of $h_1$ and the variation of the frequencies are the same.
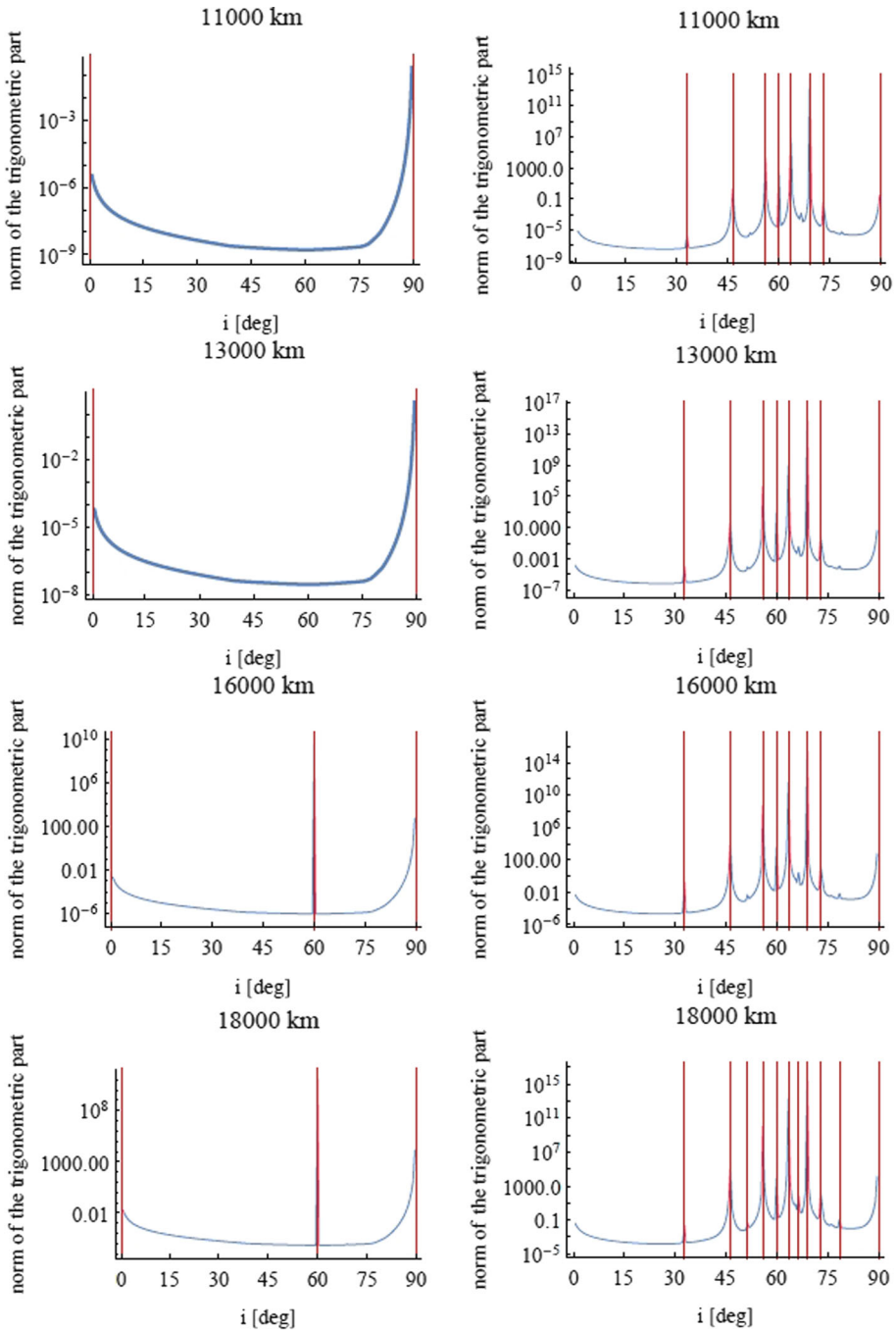
**Fig. 4** Behavior of the norm of the purely trigonometric part of $h_1$ as a function of the inclination $i_*$ for different semimajor axes and eccentricities (left: $e = 0$, right: $e = 0.5$). The red lines represent the inclinations of the resonances (see Table 2)
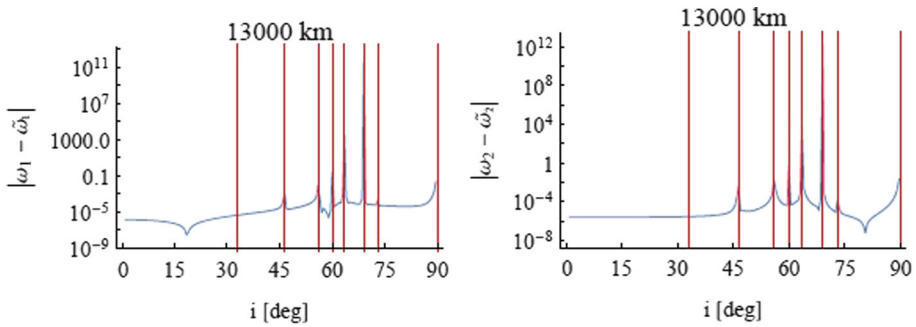
**Fig. 5** Variation between the initial ($\omega_1$ and $\omega_2$) and the final ($\tilde{\omega}_1$ and $\tilde{\omega}_2$) frequencies as a function of the inclination $i_*$ for $a = 13\,000$ km and $e_* = 0.2$. The red lines represent the values of $i_*$ associated with the resonances which affect the convergence of the normalization algorithm (see Fig. 4)

**Table 3** Comparison between the order $N(i_*)$ of the nearest resonance and the computed cut-off value $\bar{K}$, computed for $a = 13\,000$ km and $e = 0.1$

| $i_*(deg)$ | $N(i_*)$ | $\bar{K}$ | $i_*(deg)$ | $N(i_*)$ | $\bar{K}$ | $i_*(deg)$ | $N(i_*)$ | $\bar{K}$ | $i_*(deg)$ | $N(i_*)$ | $\bar{K}$ |
|---|---|---|---|---|---|---|---|---|---|---|---|
| 46.5 | 1 | 0 | 89.5 | 1 | 0 | 1 | 2 | 1 | 63.5 | 2 | 0 |
| 33 | 3 | 2 | 73 | 3 | 0 | 56 | 3 | 0 | 38 | 3 | 3 |
| 53 | 4 | 1 | 78.5 | 4 | 3 | 40.5 | 4 | 5 | 27 | 5 | 4 |
| 51.5 | 5 | 4 | 58.5 | 5 | 0 | 69 | 5 | 0 | 81.5 | 5 | 4 |
| 41.5 | 6 | 5 | 50.5 | 6 | 5 | 83.5 | 6 | 4 | | | |

## 4.3 Behavior of the cut-off value $\bar{K}$

Provided that the classical normalization converges, from the definition of the cut-off value $\bar{K}$ given in Sect. 3.2, one expects that exactly at a resonance, once denoted with $N(i_*) = |\alpha| + |\beta|$ its order, one has $\bar{K} = N(i_*) - 1$. Since in this work the inclinations are selected in a mesh of $[0, 89.5°]$ with step $0.5°$, the computations of the quantities involved in Theorem 2, including $\bar{K}$, are not performed exactly at resonance (with the exception of $i_* = 60°$, whose distance from the exact resonance is of the order of $10^{-3}$): Table 3 shows the value of $\bar{K}$ computed for the points of the mesh which are near to the resonances up to order 6, with $a = 13\,000$ km and $e = 0.1$, along with the resonance order $N(i_*)$ of the nearest one. With the exception of the inclinations associated with resonances which affect the convergence of the classical normalization, the majority of the listed inclinations follows the expected rule $\bar{K} = N(i_*) - 1$, while some slight deviation is probably due to the numerical computation.

To conclude, Fig. 6 shows the relation between the computed values of $\bar{K}$ and $|f_\epsilon|_{a,s_0,r_0}$ for $a = 13\,000$ km, $e_* = 0.2$ and $i_* \in [0, 90°]$. As expected, the cut-off decreases exponentially with the norm of the perturbing function.

## 5 Effect of higher order geopotential terms

The results of Sect. 4 were obtained by considering as basic model for MEO the one based on the $J_2$ geopotential terms. It is well known that for the lowermost altitude at MEO ($a = 10\,000$ km), the secular dynamics is shaped by higher order terms (e.g., $J_2^2$) as well as higher

**Fig. 6** Plot in $Log Log$ scale of the points $\{|f_\epsilon|_{A,r_0,s_0}, \bar{K}\}$ for $a = 13\,000$ km, $e_* = 0.2$ and $i_* \in [0, 90°]$ on a mesh of step $0.5°$
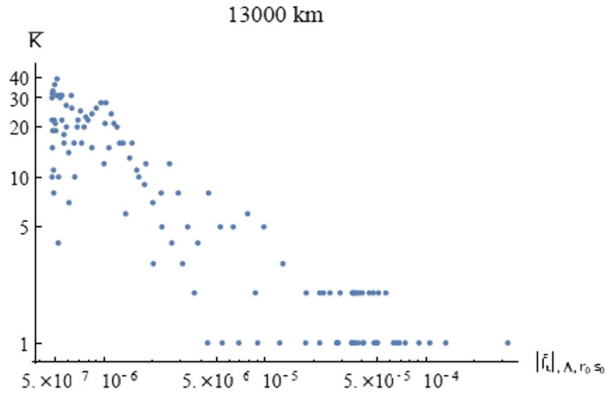


harmonics in the Earth's geopotential. In the present section, we examine a model in which the $J_2^2$ terms obtained by second-order averaging of the $J_2$ Hamiltonian term with respect to the particle's mean anomaly, as well as the first order averaging with respect to the $J_3$ and $J_4$ terms, are considered. The Hamiltonian is now as in Eq. (10), but with

$$\mathcal{H}_E^{(av)} = \mathcal{H}_{kep}^{(av)} + \mathcal{H}_{J_2}^{(av)} + \mathcal{H}_{J_3}^{(av)} + \mathcal{H}_{J_4}^{(av)} + \mathcal{H}_{J_2^2}^{(av)}, \tag{54}$$

where

$$\mathcal{H}_{J_3}^{(av)} = J_3 \frac{3\mu_E R_E^3 e \sin i}{2a^4(1-e^2)^{5/2}} \left(1 - \frac{5}{4}\sin^2 i\right)\sin(g)$$

$$\mathcal{H}_{J_4}^{(av)} = J_4 \frac{3\mu_E R_E^4}{8a^5(1-e^2)^{7/2}} \left(-1 - \frac{3e^2}{2} + \left(5 + \frac{15e^2}{2}\right)\sin^2 i\right.$$

$$\left. - \frac{35}{8}\left(1 + \frac{3e^2}{2}\right)\sin^4 i - \frac{15e^2 \sin^2 i}{4}\left(1 - \frac{3\sin^2 i}{2}\right)\cos(2g)\right),$$

while

$$\mathcal{H}_{J_2^2}^{(av)} = -J_2^2 \frac{3\mu_E R_E^4}{8a^5(1-e^2)^{7/2}} \left[\frac{5}{2} + \eta - \frac{1}{2}\eta^2 - \left(5 + 3\eta - \frac{1}{2}\eta^2\right)\sin^2 i\right.$$

$$+ \left(\frac{35}{16} + \frac{9}{4}\eta + \frac{5}{16}\eta^2\right)\sin^4 i - \left(\left(\frac{15}{4}(1+\eta) - \frac{23}{4}\eta^2 - \frac{7}{4}\eta^3\right)\sin^2 i\right.$$

$$\left. + \left(\frac{35}{8}(1-\eta) + \frac{55}{8}\eta^2 + \frac{15}{8}\eta^3\right)\sin^4 i\right)\frac{\cos(2g)}{1+\eta}\right]$$

with $\eta = \sqrt{1-e^2}$.

The Hamiltonian (54) can be obtained directly by eliminating the small body's mean anomaly through a Lie canonical transformation performed in two stages, as indicated in Deprit (1982) (see Lara 2021 for details): in the first stage, called the *elimination of the parallax*, the Hamiltonian is transformed into a function of the form

$$\mathcal{H}^{(el)} = \mathcal{H}_{kep} + \frac{1}{r^2}\left(h_{J_2}^{(el)}(a, e, i, g, h)\right.$$

$$\left. + h_{J_3}^{(el)}(a, e, i, g, h) + h_{J_4}^{(el)}(a, e, i, g, h) + h_{J_2^2}^{(el)}(a, e, i, g, h)\right),$$

thus reducing the dependence of the Hamiltonian on the small body's mean anomaly $M$ in only the factor $1/r^2$. In the second stage, we then eliminate this dependence with the usual procedure of Delaunay normalization (Palacián 2002). It should be stressed that this procedure yields equivalent results for the terms $\mathcal{H}_{J_2}^{(av)}$, $\mathcal{H}_{J_3}^{(av)}$ and $\mathcal{H}_{J_4}^{(av)}$ as the simple *scissor averaging* of Eq. (12), but it allows to formally introduce terms of higher order as $\mathcal{H}_{J_2^2}^{(av)}(a, e, i, g, h)$. Also, an important difference is in the physical interpretation, since the Lie transformation, which is a near to identity transformation mapping the original canonical variables to new ones, still contains short-periodic terms, even while the Hamiltonian does not. In the jargon of astrodynamics, this is called a transformation from *osculating* to *mean elements*. As already pointed out in Sect. 2.2, this means that, formally, all the results on Nekhoroshev stability in this and in previous sections refer to the stability of the mean elements, while the osculating elements perform short-period bounded oscillations around the secularly evolving values of the mean elements.

Returning to the latter question, Fig. 7 allows to compare the results on Nekhoroshev stability using the Hamiltonian (10) with $\mathcal{H}_E^{(av)}$ computed as in (54), with those of the simple $J_2$-only model obtained as in (12).

Figure 7 provides information on both the domain of applicability of the Nekhoroshev theorem as well as the corresponding stability times: we consider the case of orbits with $e = 0.3$ and two different values of the semimajor axis, namely $a = 11000$ km (top panel in Fig. 7) and $a = 17000$ km (middle panel). The abscissa of each of the marked points indicates a value of the inclination for which applying Pöschel's theorem in the form of the algorithm of Sect. 3.2 yields a positive result, i.e., that the Nekhoroshev stability criterion holds. The ordinate then indicates the corresponding time of Nekhoroshev stability. From these figures stem the following remarks:

(i) the two models (simple $J_2$ and 'extended') yield practically identical *domains* of stability. This is to be expected, since the domains of stability are mostly determined by the values of the (Diophantine) frequencies of the integrable part of the Hamiltonian $H_0$. In the extended model, the frequencies differ from those of the $J_2$−model by the addition of the terms $O(J_2^2)$, $O(J_3)$ and $O(J_4)$. All these terms are about $10^{-3}$ the size of the leading ($J_2$) terms; thus, they only affect the frequencies at the third digit. This implies, in turn, that all Diophantine constants, cut-off in Fourier space etc., entering into the application of Pöschel's theorem remain practically invariant in computations with the extended model.

(ii) On the other hand, the computed *times* of Nekhoroshev stability change, by about one order of magnitude at the lowest limit of the MEO zone ($a = 11\,000$ km), and marginally as we approach the limit of the overall loss of the Nekhoroshev stability in Pöschel's sense $a > 17\,000$ km. The main reason for this difference lies in the integrability of the $J_2$ averaged model, which implies that only lunisolar perturbations affect the size of the term $H_1$ in the Hamiltonian of the simple $J_2$ model. In the extended model, instead, all three $O(J_2^2)$, $O(J_3)$ and $O(J_4)$ terms contribute to $H_1$ due to their containing $\cos(2g)$ and $\sin(g)$ terms depending on the canonical angles. It is noteworthy that the relative importance of these terms decreases as a power of the semimajor axis [see Eq. (54)], while the lunisolar perturbations increase with $a$, e.g. as $a^2$ for the quadrupolar terms. In particular, we find that the $\cos(2g)$ term due to $J_2^2$ and $J_4$ is dominant over the $\cos(2g)$ term generated by the lunisolar perturbation when $a = 11000$ km, but the former is only about 1.5% the size of the latter when $a = 20\,000$ km. As a result, the two different models converge as regards the times of stability as $a$ increases, a tendency shown clearly in the bottom panel of Fig. 7.

**Fig. 7** Comparison of the domains and times of Nekhoroshev stability for different values of the inclination between the $J_2$ model (yellow dots) and the model including $J_2^2$, $J_3$, $J_4$ (blue dots), for a fixed eccentricity $e = 0.3$ and semimajor axis equal to $a = 11\,000$ km (top panel), or $a = 17\,000$ km (middle panel). A colored point indicates that Pöschel's criterion for Nekhoroshev stability is satisfied at the corresponding value of the inclination, shown in the abscissa. The ordinate shows the corresponding value of the Nekhoroshev stability time (in years). Bottom panel: comparison of the Nekhoroshev stability times as a function of the semimajor axis $a$ in the $J_2$ model and in the extended model for $e = 0.3$ and $i = 20^o$
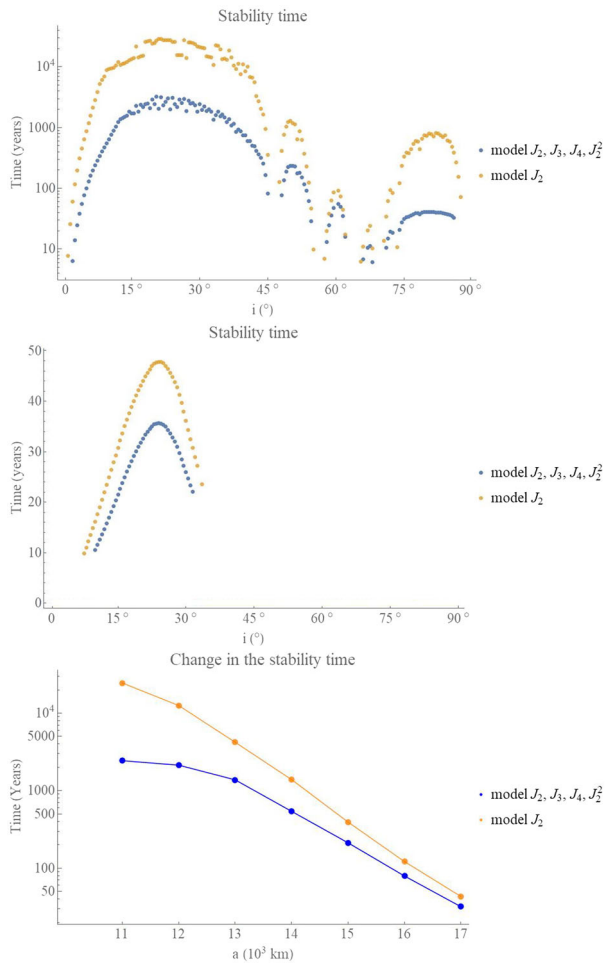


At any rate, it is important to note that in both models, the computed times of stability correspond to $10^7$ orbital revolutions in the lowermost limit of the MEO zone, reducing to about $10^5$ orbital revolutions in the highermost limit where Nekhoroshev stability holds. These times are thus quite consistent with applications of the Nekhoroshev theorem in the practical context of the long-term stability of satellite orbits, as they are larger by orders of magnitude compared to the satellites' operational lifetime.

## 6 Conclusions

Our work in the present paper has a twofold aim: on one side, we provide a specific algorithm by which we are able to formally specify the domains in the space of orbital elements $(a, e, i)$ for which Nekhoroshev stability holds in the sense that all the necessary conditions for the applicability of Pöschel's theorem for non-resonant orbits are satisfied. On the other side, in those domains where Nekhoroshev stability holds, we compute the associated Nekhoroshev

times and demonstrate that these times are long enough to be of use in practical Earth satellite applications. Our main results can be summarized as follows:

1. We examine in detail a secular model based on a 'scissor' averaged Hamiltonian over the fast angles, including the term $J_2$ as well as lunisolar perturbations. For this model, we propose: (i) a detailed 'book-keeping' algorithm allowing to write the Hamiltonian in a form suitable for the application of Pöschel's theorem, and (ii) a 'preliminary normalization', which leads to a model devoid of the effects of trigonometric terms generated by the shifting of the secular equilibrium from the Earth's equator to the Laplace plane. Albeit technical, this step (analyzed in detail in Sect. 2.4) turns to be crucial in suitably engineering the Hamiltonian so that relevant estimates on the real size of the secular perturbations can be obtained.

2. We then propose, in subsection 3.2, a particular algorithm by which the theorem of Pöschel can be transformed into a binary ("yes" or "no") criterion for the holding of Nekhoroshev stability in a small domain around any preselected value of the elements $(a, e, i)$ within the MEO zone. Implementing this algorithm leads to the results of Fig. 1: as intuitively expected, we find that the domains of Nekhoroshev stability shrink as the altitude (semimajor axis $a$) increases. This is due to the growing size of lunisolar perturbations as $a$ increases. The most robust domain is found in the intervals $0 \leq e \leq 0.3$ and $10° \leq i \leq 30°$; the latter interval roughly corresponds to a domain well protected from major inclination-only dependent lunisolar resonances.

3. Using the same algorithm we can compute the times of Nekhoroshev stability, which span from $10^5$ to $10^7$ satellite orbital periods. These times are sufficiently high for applications related to the operational lifetime and end-of-life deployment of satellites, as well as to the long-term orbital evolution of populations of space debris.

4. Finally, we examine a more extended model including the $J_3$ and $J_4$ harmonics of the Earth's potential as well as $J_2^2$ terms obtained by second-order averaging of the Hamiltonian in closed form. While the complexity of the new model renders a full investigation of this extended model beyond our present scope, we provide some key comparisons with our basic (only $J_2$) model: (i) the domains of stability remain practically the same in the two models, while (ii) the times of stability are affected by about one order of magnitude at the lowermost limit of the MEO zone, a difference tending nevertheless to vanish as $a$ increases. Section 5 discusses in detail the origin for these differences.

We should emphasize again that our study was limited only to the case in which the frequencies of motion satisfy suitable non-resonant conditions. Another limitation is that we disregarded the slow precession of the lunar nodes with respect to the ecliptic plane, by simply considering a constant inclination of the Moon, equal to the one of the ecliptic. Notwithstanding the arguments presented in Sect. 2 as regards the precision of this model (presently motivated mostly by our computational limits), we still emphasize that we consider the results of this work as a first step that paves the way to several future directions of research. Among possible future extensions, we indicate: (i) exploring the application of the resonant Nekhoroshev's theorem, which becomes relevant for particular values of the inclination associated with lunisolar resonances, and (ii) removing the assumption of a fixed ellipse for the Moon's orbit. These possibilities leave open that Nekhoroshev stability might actually hold in domains larger than the ones found in the present work, extending to altitudes $a > 18,000$ km were many satellites reside (e.g., GPS and geosynchronous satellites).

As a final remark, we note that the approach followed in the present paper, based on applying the Nekhoroshev theorem, is advantageous over other approaches to the stability problem also in the sense of being directly extendable to Hamiltonian models with more than

two degrees of freedom (as opposed, for example, to approaches as the Lyapunov or KAM stability in the sense of confinement between invariant tori), as well as in the case of initial conditions close to resonances. In this sense, we anticipate that the technique presented in the current paper could prove useful also in the context of more general problems encountered in the area of astrodynamics.

**Data Availability** The datasets generated during and/or analyzed during the current study are available from the corresponding author on reasonable request.

## Declarations

**Conflict of interest** The author A.C. is Editor-in-Chief of the journal "Celestial Mechanics and Dynamical Astronomy"; the paper underwent a standard single-blind peer review process.

## Appendix A.: Analytical expressions of $\mathcal{H}_b^{(av)}$ and $\mathcal{H}^{(sec)}$ in Sect. **2**

### A.1 Expansion of $\mathcal{H}_b^{(av)}$

We provide an expression of $\mathcal{H}_b^{(av)}$ for a third body (index $b$, referring to the Moon or Sun) as a function of its orbital parameters $(a_b, e_b, i_b, \omega_b, \Omega_b)$ and the debris' parameters $(a, e, i, \omega, \Omega)$. Up to second order in the eccentricity, we have:

$$
\begin{aligned}
\mathcal{H}_b^{(av)} = {} & \frac{a^2}{16a_b^3(1-e_b^2)^{3/2}} \bigg( -\frac{2+3e^2}{8}(1+3\cos(2i))(1+3\cos(2i_0)) \\
& -\frac{15}{4}e^2(1+3\cos 2i_0)\sin i^2 \cos 2\omega - \frac{3}{2}(2+3e^2)\sin i^2 \sin i_0{}^2 \cos 2(\Omega - \Omega_{b_0}) \\
& -15e^2\cos(i/2)^4 \sin i_0{}^2 \cos 2(\omega + \Omega - \Omega_{b_0}) - \frac{3}{2}(2+3e^2)\sin(2i)\sin(2i_0) \\
& \cos(\Omega - \Omega_{b_0}) + 30e^2 \cos(i/2)^3 \sin(i/2)\sin(2i_0)\cos(2\omega + \Omega - \Omega_{b_0}) \\
& +\frac{15}{2}e^2(-1+\cos i)\sin i \sin i_0 \cos(2\omega - \Omega + \Omega_{b_0}) \\
& -15e^2 \sin(i/2)^4 \sin(i_0)^2 \cos 2(\omega - \Omega + \Omega_{b_0}) \bigg).
\end{aligned}
\tag{55}
$$

## A.2 List of the nonzero terms in $\mathcal{H}^{(sec)}$ for $j = 1, 2$

Assuming, as in Sect. 2, that both the lunar and solar orbits lie on a fixed ecliptic plane inclined with respect to the Earth's equatorial plane by an angle $i_0$, the frequencies $\omega_1$ and $\omega_2$ appearing in (17) are given by:

$$\omega_1 = \omega_1^{(J_2)} + \omega_1^{(M)} + \omega_1^{(\odot)}, \qquad \omega_2 = \omega_2^{(J_2)} + \omega_2^{(M)} + \omega_2^{(\odot)},$$

where

$$\omega_1^{(J_2)} = -\frac{3}{4} R_E^2 J_2 \mu_E^4 \frac{(-1 + 5 \cos i_*{}^2 - 2 \cos i_*)}{(\mu_E a)^{7/2}(1 - e_*^2)^2}$$

$$\omega_2^{(J_2)} = \frac{3}{2} \frac{R_E^2 J_2 \mu_E^4}{(\mu_E a)^{7/2}(1 - e^2)^2} \cos i_*$$

$$\omega_1^{(M/\odot)} = -\frac{3}{64} a^{3/2} \mu_{M/\odot} \frac{[3 + 2e_*^2 - 2(2 + 3e_*^2)\cos i_* + 5 \cos 2i_*](1 + 3 \cos 2i_0)}{\sqrt{1 - e_*^2}\sqrt{\mu_E}(a_{M/\odot}(1 - e_{M/\odot}))^3}$$

$$\omega_2^{(M/\odot)} = \frac{3}{32} a^{3/2} \mu_{M/\odot} \frac{(2 + 3e_*^2)\cos i_* (1 + 3 \cos 2i_0)}{\sqrt{1 - e_*^2}\sqrt{\mu_E}\left(a_{M/\odot}(1 - e_{M/\odot})\right)^3}. \tag{56}$$

The coefficients $a_{\mathbf{l}}$ and $b_{\mathbf{l},\mathbf{k}}$ in (22) are given by:

$$a_{(2,0)} = \frac{3}{4} \frac{J_2 R_E^2}{a^4(1 - e_*^2)^{5/2}}(1 + 10 \cos i_* - 15 \cos^2 i_*) +$$

$$-\frac{3}{128} \frac{a}{\mu_E(1 - e_*^2)}\left(\frac{\mu_M}{R_M^3} + \frac{\mu_\odot}{R_\odot^3}\right)(1 + 3 \cos 2i_0)(21 + 4e_*^2 - 40 \cos i_* + 15 \cos 2i_*)$$

$$a_{(1,1)} = \frac{3}{2} \frac{J_2 R_E^2}{a^4(1 - e_*^2)^{5/2}}(5 \cos i_* - 1) +$$

$$-\frac{3}{32} \frac{a}{\mu_E(1 - e_*^2)}\left(\frac{\mu_M}{R_M^3} + \frac{\mu_\odot}{R_\odot^3}\right)(1 + 3 \cos 2i_0)(2 + 3e_*^2 - 10 \cos i_*)$$

$$a_{(0,2)} = -\frac{3}{4} \frac{J_2 R_E^2}{a^4(1 - e_*^2)^{5/2}} +$$

$$-\frac{3}{64} \frac{a}{\mu_E(1 - e_*^2)}\left(\frac{\mu_M}{R_M^3} + \frac{\mu_\odot}{R_\odot^3}\right)(1 + 3 \cos 2i_0)\left(2 + 3e_*^2\right)$$

$$b_{(0,0),(\pm2,0)} = -\frac{15}{32}(a^2 e_*^2 \sin^2 i_0 \cos^4(i_*/2))\left(\frac{\mu_M}{r_M^3} + \frac{\mu_\odot}{r_\odot^3}\right)$$

$$b_{(0,0),(\pm2,\pm1)} = \frac{15}{16}\left[a^2 e_*^2 \sin(2i_0)\cos^3(i_*/2)\sin(i_*/2)\right]\left(\frac{\mu_M}{r_M^3} + \frac{\mu_\odot}{r_\odot^3}\right)$$

$$b_{(0,0),(\pm2,\mp2)} = -\frac{15}{128}\left[a^2 e_*^2(i + 3\cos(2i_0))\sin^2 i_*\right]\left(\frac{\mu_M}{r_M^3} + \frac{\mu_\odot}{r_\odot^3}\right)$$

$$b_{(0,0),(\pm2,\mp3)} = -\frac{15}{16}\left[a^2 e_*^2 \sin(2i_0)\sin^3(i_*/2)\cos(i_*/2)\right]\left(\frac{\mu_M}{r_M^3} + \frac{\mu_\odot}{r_\odot^3}\right)$$

$$b_{(0,0),(\pm2,\mp4)} = -\frac{15}{32}\left[a^2 e_*^2 \sin^2 i_0 \sin^4(i_*/2)\right]\left(\frac{\mu_M}{r_M^3} + \frac{\mu_\odot}{r_\odot^3}\right)$$

$$b_{(0,0),(0,\pm1)} = -\frac{3}{64}\left[a^2(2 + 3e_*^2)\sin(2i_0)\cos(2i_*)\right]\left(\frac{\mu_M}{r_M^3} + \frac{\mu_\odot}{r_\odot^3}\right)$$

$$b_{(0,0),(0,\pm2)} = -\frac{3}{64}\left[a^2(2 + 3e_*^2)\sin^2 i_0 \sin^2 i_*\right]\left(\frac{\mu_M}{r_M^3} + \frac{\mu_\odot}{r_\odot^3}\right).$$

## References

Alessi, E.M., Deleflie, F., Rosengren, A., Rossi, A., Valsecchi, G., Daquin, J., Merz, K.: A numerical investigation on the eccentricity growth of GNSS disposal orbits. Celest. Mech. Dyn. Astron. **125**(1), 71–90 (2016)

Aristoff, J., Horwood, J., Alfriend, K.: On a set of $J_2$ equinoctial orbital elements and their use for uncertainty propagation. Celest. Mech. Dyn. Astron. **133**(9), 1–9 (2021)

Arnold, V.: Instability of dynamical systems with several degrees of freedom. Sov. Math. Doklady **5**, 581–585 (1964)

Benettin, G., Gallavotti, G.: Stability of motions near resonances in quasi-integrable Hamiltonian systems. J. Stat. Phys. **44**(3–4), 293–338 (1986)

Breiter, S.: Lunisolar resonances revisited. Celest. Mech. Dyn. Astron. **81**, 81–91 (2001)

Breiter, S.: On the coupling of lunisolar resonances for Earth satellite orbits. Celest. Mech. Dyn. Astron. **80**(1), 1–20 (2001)

Brouwer, D.: Solution of the problem of artificial satellite theory without drag. Astron. J. **64**, 378–397 (1959)

Casanova, D., Petit, A., Lemaître, A.: Long-term evolution of space debris under the $J_2$ effect, the solar radiation pressure and the solar and lunar perturbations. Celest. Mech. Dyn. Astron. **123**, 223–238 (2015)

Celletti, A.: Stability and Chaos in Celestial Mechanics. Springer, Berlin (2010) (published in association with Praxis Publishing, Chichester)

Celletti, A., Ferrara, L.: An application of Nekhoroshev theorem to the restricted three-body problem. Celest. Mech. Dyn. Astron. **64**, 261–272 (1996)

Celletti, A., Gales, C.: On the dynamics of space debris: 1:1 and 2:1 resonances. J. Nonlinear Sci. **24**(6), 1231–1262 (2014)

Celletti, A., Galeş, C.: Dynamics of resonances and equilibria of low Earth objects. SIAM J. Appl. Dyn. Syst. **17**(1), 203–235 (2018)

Celletti, A., Giorgilli, A.: On the stability of the Lagrangian points in the spatial restricted problem of three bodies. Celest. Mech. Dyn. Astron. **50**, 31–58 (1991)

Celletti, A., Gales, C., Pucacco, G.: Bifurcation of lunisolar secular resonances for space debris orbits. SIAM J. Appl. Dyn. Syst. **15**, 1352–1383 (2016)

Celletti, A., Efthymiopoulos, C., Gachet, F., Galeş, C., Pucacco, G.: Dynamical models and the onset of chaos in space debris. Int. J. Non-Linear Mech. **90**, 147–163 (2017)

Celletti, A., Gales, C., Pucacco, G., Rosengren, A.: Analytical development of the lunisolar disturbing function and the critical inclination secular resonance. Celest. Mech. Dyn. Astron. **127**(3), 259–283 (2017)

Celletti, A., Gales, C., Lhotka, C.: Resonances in the Earth's space environment. Comm. Nonlinear Sci. Numer. Simul. **84**, 105185 (2020)

Chao, C., Gick, R.: Long-term evolution of navigation satellite orbits: GPS/GLONASS/GALILEO. Adv. Space Res. **34**, 1221–1226 (2004)

Cook, G.E.: Luni-solar perturbations of the orbit of an Earth satellite. Geophys. J. Int. **6**(3), 271–291 (1962)

Daquin, J., Rosengren, A., Alessi, E., Deleflie, F., Valsecchi, G., Rossi, A.: The dynamical structure of the MEO region: long-term stability, chaos, and transport. Celest. Mech. Dyn. Astron. **124**(4), 335–366 (2016)

De Blasi, I., Celletti, A., Efthymiopoulos, C.: Semi-analyitical estimates for the orbital stability of Earth's satellite. J. Nonlinear Sci. **31**(93), 1–37 (2021)

Deprit, A.: Delaunay Normalisations. Celest. Mech. **26**(1), 9–21 (1982)

Ely, T., Howell, K.: Dynamics of artificial satellite orbits with tesseral resonances including the effects of luni-solar perturbations. Dyn. Stab. Syst. **12**(4), 243–269 (1997)

Giacaglia, G.: Lunar perturbations of artificial satellites of the Earth. Celest. Mech. **9**, 239–267 (1974)

Giorgilli, A., Skokos, C.: On the stability of the Trojan asteroids. Astron. Astrophys. **317**, 254–261 (1997)

Gkolias, I., Daquin, J., Gachet, F., Rosengren, A.: From order to chaos in Earth satellite orbits. Astron. J. **152**(5), 119 (2016)

Hughes, S.: Earth satellite orbits with resonant lunisolar perturbations. I. Resonances dependent only on inclination. Proc. R. Soc. Lond. A **372**, 243–264 (1980)

Kaula, W.: Development of the lunar and solar disturbing functions for a close satellite. Astron. J. **67**, 300–303 (1962)

Lane, M.T.: On analytic modeling of lunar perturbations of artificial satellites of the Earth. Celest. Mech. Dyn. Astr. **46**(4), 287–305 (1989)

Lara, M.: *Hamiltonian Perturbation Solutions for Spacecraft Orbit Prediction.* De Gruyter Studies in Mathematical Physics (2021)

Lara, M., San-Juan, J.F., López-Ochoa, L.M.: Delaunay variables approach to the elimination of the perigee in artificial satellite theory. Celest. Mech. Dyn. Astron. **120**(1), 39–56 (2014)

Lara, M., López, R., Pérez, I., San-Juan, J.F.: Exploring the long-term dynamics of perturbed keplerian motion in high degree potential fields. Commun. Nonlinear Sci. Numer. Simul. **82**, 105053 (2020)

Lemaître, A., Delsate, N., Valk, S.: A web of secondary resonances for large $A/m$ geostationary debris. Celest. Mech. Dyn. Astron. **104**, 383–402 (2009)

Lhotka, C., Celletti, A., Gales, C.: Poynting-Robertson drag and solar wind in the space debris problem. Mon. Not. R. Astron. Soc. **460**, 802–815 (2016)

Nekhoroshev, N.: An exponential estimate of the time of stability of nearly-integrable Hamiltonian systems. Uspekhi Matematicheskikh Nauk **32**(6), 5–66 (1977)

Nie, T., Gurfil, P.: Long-term evolution of orbital inclination due to third-body inclination. Celest. Mech. Dyn. Astron. **133**(1), 1–33 (2021)

Palacián, J.: Normal forms for perturbed keplerian systems. J. Differ. Equ. **180**(2), 471–519 (2002)

Pöschel, J.: Nekhoroshev estimates for quasi-convex Hamiltonian systems. Math. Z. **213**(1), 187–216 (1993)

Rosengren, A., Scheeres, D.: Long-term dynamics of high area-to-mass ratio objects in high-Earth orbit. Adv. Space Res. **52**, 1545–1560 (2013)

Rosengren, A., Alessi, E., Rossi, A., Valsecchi, G.: Chaos in navigation satellite orbits caused by the perturbed motion of the moon. Mon. Not. R. Astron. Soc. **449**, 3522–3526 (2015)

Rosengren, A., Daquin, J., Tsiganis, K., Alessi, E., Deleflie, F., Rossi, A., Valsecchi, G.: Galileo disposal strategy: stability, chaos and predictability. Mon. Not. R. Astron. Soc. **464**(4), 4063–4076 (2016)

Rossi, A.: Resonant dynamics of medium Earth orbits: space debris issues. Celest. Mech. Dyn. Astron. **100**(4), 267–286 (2008)

Skoulidou, D., Rosengren, A., Tsiganis, K., Voyatzis, G.: Medium Earth orbit dynamical survey and its use in passive debris removal. Adv. Space Res. **63**(11), 3646–3674 (2019)

Valk, S., Lemaître, A.: Analytical and semi-analytical investigations of geosynchronous space debris with high area-to-mass ratios. Adv. Space Res. **41**, 1077–1090 (2008)